Geochemical Journal, Vol. 39, pp. 547 to 571, 2005

New chemical and original isotopic data on waters from El Tatio geothermal field, northern Chile

GIANNI CORTECCI,[1]* TIZIANO BOSCHETTI,[2] MARIO MUSSI,[1] CHRISTIAN HERRERA LAMELI,[3] CLAUDIO MUCCHINO[4] and MAURIZIO BARBIERI[5]

[1]Istituto di Geoscienze e Georisorse, Area della Ricerca CNR, Via Moruzzi 1, I-56124 Pisa, Italy
[2]Dipartimento di Scienze della Terra, University of Parma, Parco Area delle Scienze 157/A, I-43100 Parma, Italy
[3]Departamento de Ciencias Geológicas, Universidad Católica del Norte, Avenida Angamos 0610, Antofagasta, Chile
[4]Dipartimento di Chimica Generale ed Inorganica, Chimica Analitica, Chimica Fisica, University of Parma, Parco Area delle Scienze 17A, I-43100, Parma, Italy
[5]Dipartimento di Scienze della Terra, "La Sapienza" University of Roma, Piazzale Aldo Moro 5, I-00185 Roma, Italy

(*Received December 1, 2004; Accepted June 1, 2005*)

The El Tatio geothermal field is located at an height of 4200–4300 m on the Cordillera de los Andes (Altiplano). Geysers, hot pools and mudpots in the geothermal field and local meteoric waters were sampled in April 2002 and analyzed for major and trace elements, δ^2H, δ^{18}O and ^{3}H of water, δ^{34}S and δ^{18}O of dissolved sulfate, δ^{13}C of dissolved total carbonate, and ^{87}Sr/^{86}Sr ratio of aqueous strontium.

There are two different types of thermal springs throughout the field, that are chloride-rich water and sulfate-rich water. The chemical composition of chloride springs is controlled by magma degassing and by water-rock interaction processes. Sulfate springs are fed by shallow meteoric water heated by ascending gases. In keeping with the geodynamic setting and nature of the reservoir rocks, chloride water is rich in As, B, Cs, Li; on the other hand, sulfate water is enriched only in B relative to local meteoric water.

Alternatively to a merely meteoric model, chloride waters can be interpreted as admixtures of meteoric and magmatic (circa andesitic) water, which moderately exchanges oxygen isotopes with rocks at a chemical Na/K temperature of about 270°C in the main reservoir, and then undergoes loss of vapor (and eventually mixing with shallow water) and related isotopic effects during ascent to the surface. These chloride waters do not present tritium and can be classified as sub-modern (pre-1952). A chloride content of 5,400 mg/l is estimated in the main reservoir, for which δ^2H and δ^{18}O values, respectively of –78‰ and –6.9‰, are calculated applying the multistage-steam separation isotopic effects between liquid and vapor. From these data, the meteoric recharge (Cl ≈ 0 mg/l) of the main reservoir should approach a composition of –107‰ in δ^2H and –14.6‰ in δ^{18}O, when a magmatic water of δ^2H = –20‰, δ^{18}O = +10‰ and Cl = 17,500 mg/l is assumed.

The ^{87}Sr/^{86}Sr ratios of the hot springs are quite uniform (0.70876 to 0.70896), with values within the range observed for dacites of the Andean central volcanic zone. A water δ^{18}O-^{87}Sr/^{86}Sr model was developed for the main geothermal reservoir, by which a meteoric-magmatic composition of the fluids is not excluded.

The uniform δ^{34}S(SO_4^{2-}) values of +1.4 to +2.6‰ in the chloride waters agree with a major deep-seated source for sulfur, possibly via hydrolysis in the geothermal reservoir of sulfur dioxide provided by magma degassing, followed by isotopic exchange between sulfate and sulfide in the main reservoir. This interpretation is supported by the largely negative δ^{34}S(SO_4^{2-}) value in steam-heated water sulfate (–9.8‰) and mass-balance calculation, which exclude leaching at depth of igneous iron-sulfides with δ^{34}S near zero per mill.

All the δ^{13}C values of total carbonate in the chloride waters are negative, with variable values from –9.2 to –20.1‰, pointing to an important proportion of biogenic carbon in the fluids. The interpretation of these data is problematic, and a number of alternative explanations are reported in the text.

Keywords: trace elements, isotope geochemistry, andesitic water, El Tatio geothermal field, Chile

INTRODUCTION

Based on previous investigations by Ellis (1969), Cusicanqui *et al*. (1975) and Giggenbach (1978), hot springs (geysers, spouting pools, mudpots) and well waters (down to 733 m) from El Tatio geothermal field include high chloride waters to the north, low chloride waters to the south-west, chloride-bicarbonate waters to the north, and sulfate-bicarbonate waters to west and east. Many of the chloride waters are at or near to the local boiling point of 86°C. A collection of data on the oxygen

*Corresponding author (e-mail: g.cortecci@igg.cnr.it)

and hydrogen isotope composition of these waters can be found in Giggenbach (1978); it refers to samples collected during November 1968 to March 1971, between 31 and 34 years before our sampling campaign in April 2002.

Chemical and isotopic data on thermal waters from 1968 to 1971 were combined by Giggenbach (1978) in order to inquire into the origin of El Tatio geothermal system. A variety of processes and discharges were recognized: (1) dilution of primary high chloride geothermal water (5500 mg/l; 260°C) with local groundwater produces secondary chloride water (4750 mg/l; 190°C), that feeds some springs within a small area; (2) single-step steam separation from these primary and secondary waters determines isotopic shifts and increases the chloride contents to 8000 and 6000 mg/l, respectively; (3) absorption of steam and carbon dioxide into local groundwater and mixing with shallow chloride water leading to the formation of high total alkalinity, low chloride waters (160°C); and (4) absorption of H_2S-bearing steam into surface water and the formation of high sulfate waters with near zero chloride.

According to the hydrogeological models (Healy and Hochstein, 1973; Cusicanqui *et al*., 1975; Giggenbach, 1978; Muñoz and Hamza, 1993), meteoric waters infiltrate in recharge areas located some 15 km east from the field, heat going to the west at a rate of about 1.3 km/year, and enter the El Tatio basin from the Cerros de El Tatio, as a lateral outflow within the permeable ignimbrites of the Puripicar Formation (190 to 240 m thick) and the Salado Member (80 to 100 m thick). Thus, they feed the major aquifer of the field after about 15 years moving from east to west (Healy, 1974; Cusicanqui *et al*., 1975). The fluid is confined within these two units by the overlying impermeable Tucle Tuff subunit of the El Tatio Formation. A secondary important aquifer occurs in the permeable Tucle Dacite subunit (about 100 m thick), which is capped by the impermeable Tatio Ignimbrite subunit; the fluid in this aquifer arises from the admixture of primary fluid from the main reservoir, and ascending through local permeable channels in the underlying Tucle Tuff subunit, with cold groundwater descending through the dacite (Cusicanqui *et al*., 1975). In addition to these two major aquifers, a brine was discovered below about 600 m depth at a temperature of 190°C (well below the boiling point for depth). The origin of this brine (pH of 2 at 25°C, density of 1.2, chloride concentration of about 185,000 ppm; Cusicanqui *et al*., 1975) remains uncertain. It may derive from adsorption of magmatic steam into groundwater (Giggenbach, 1978). Otherwise, it may be a groundwater that interacted with evaporite beds (Youngman, 1984), which however were not seen in any core or cuttings drilled out.

The geothermal drillings carried out at El Tatio between 1969 and 1974 (and possibly those drilled at 30 km to the east in Bolivia at Sol de Mañana) seemed to have modified the hydrogeological features of the geothermal system, reducing substantially the number of geysers and hot springs presumably due to the lowering of the water table (Jones and Renaut, 1997; see also Cusicanqui *et al*., 1975). The main aquifer was drilled in the eastern part of the field between 800 and 1000 m depth, where a temperature of 263°C was measured (Cusicanqui *et al*., 1975); other aquifers with temperatures between 160 and 230°C were drilled at shallower depths.

The present study on El Tatio was undertaken in order to (1) verify the persistence of the geochemical features of the geothermal system, in terms of multi-aquifer structure and enthalpy of the fluids; (2) acquire original data on the sulfur, carbon and strontium isotope compositions of solutes, along with a more complete set of concentration data on trace elements in solution; (3) delineate the role of magmatic sources in providing water and elements compared to the meteoric source and water-rock interaction processes; and finally (4) elaborate an up-to-date geochemical model combining old and new chemical and isotopic results.

Study Area

The El Tatio geothermal field (22°20′ S, 68°01′ W) constitutes a volcanogenic, dynamic and liquid-dominated hydrologic system, located about 80 km to the east of Calama, in the Antofagasta Province of northern Chile (Fig. 1). Important physiographic features in the study area are the Serrania de Tucle ridge and its offset Loma Lucero. The sedimentary core of Serrania de Tucle is considered by Healy and Hochstein (1973) to act as a barrier to regional westward flow of groundwater through the volcanic formations. It is inferred that faults, associated to the Loma Lucero offset (Healy, 1974), on the south western foot of Copacoya peak (4807 m), pass through the southern part of the geothermal field, providing vertical permeability. On the other hand, the northern thermal features of the field are aligned with a north-east trending zone of faulting (Geyser Fault; Healy, 1974).

The geothermal field is located at an height of 4300 m amid andesitic stratovolcanoes of the High Andes Cordillera (e.g., El Volcán, 5560 m; Cerros de El Tatio, 5083 m; and Volcano Tatio, 5314 m), within the north-south trending "Graben El Tatio" which extends at the base of the western flank of Cerros de El Tatio. The graben is infilled by a 1000 m thick sequence of nearly horizontal ignimbrites, tuffs and lavas of Tertiary to Quaternary age, overlying a tick sequence of lapilli tuff, siltstone and breccia of Tertiary age (e.g., Lahsen and Trujillo, 1975 and references therein).

Details on the regional geology of the area can be found in Guest (1969) and De Silva (1989). Shortly, the

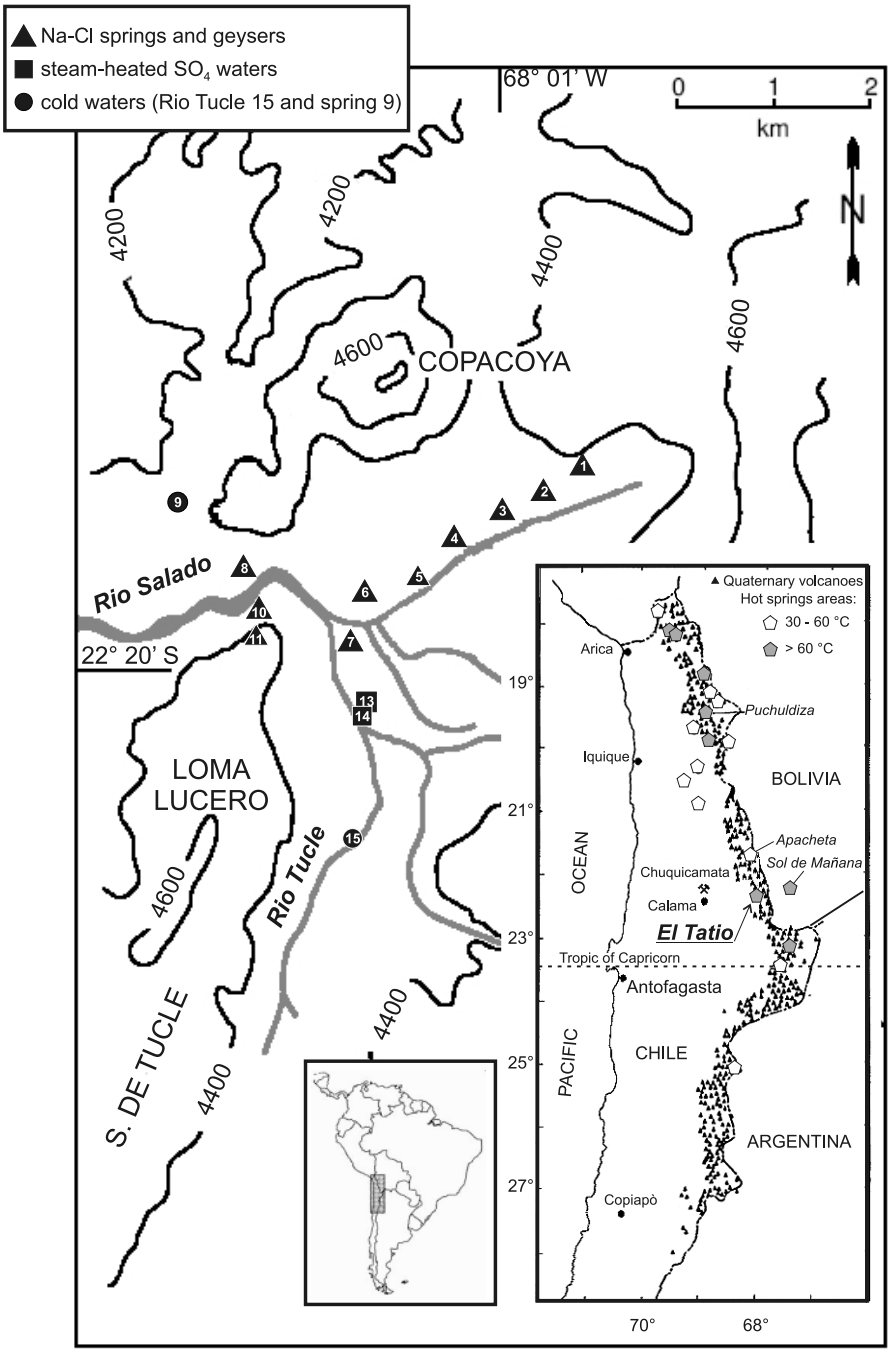

Fig. 1. Map of the El Tatio geothermal field in northern Chile, and location of the studied hot chloride (1 to 8 and 10 and 11) sulfate springs (13 and 14), and cold waters (Rio Tucle 15 and spring 9).

area consists mostly of late Miocene to middle Pliocene ignimbrites lying unconformably over Cretaceous sediments. In the late Pliocene, andesitic volcanism started and still goes on, and the produced andesites constitute the High Andes of the Cordillera.

The upper part of the basement is constituted by the Quebrada Justo Formation made up of Cretaceous sediments constituted by tuffaceous shale with sandstone and tuff bands. It is unconformably overlain by the San Bartolo Group (SBG), consisting of Miocene to Pleistocene volcanics and ignimbrites. From bottom to top, SBG includes (De Silva, 1989) the Rio Salado Member, the Sifon Member; the Puripicar Formation and the El Tatio Formation. The top of SBG borders on stratified

sands and gravels, followed by the Upper Pleistocene-Holocene lavas of the Andean Volcanics unit.

The Rio Salado Member of the Artola Formation (9.56 ± 0.48 Ma) is the oldest and thickest (over 1800 m) ignimbrite unit in the El Tatio geothermal area. The Sifon Member (Upper Miocene), of about 300 m thick in the Tatio Graben (Lahsen and Trujillo, 1975), correlates westwards with the Chiu ignimbrite and northwards with the Upper Rio San Pedro Ignimbrite (De Silva, 1989). Plagioclase and biotite in these rocks occur as essential minerals in nearly equal amounts. Lithics are rare, except at the base of the members, where pyroclastic flows travelled over loose gravels. Pumice is commonly found associated with major plagioclase and biotite; quartz is generally absent.

The Puripicar Formation (4.22 ± 0.04 Ma) is about 300 m thick in the Tatio Graben. The best exposures of this ignimbrite can be found westwards and southwards from El Tatio geothermal field. The crystal content of the moderately vesicular dacitic component is 55%, and mainly consists of plagioclase with abundant quartz, biotite, hornblende and widespread oxides.

The El Tatio Formation (Pleistocene) overlies the Puripicar Formation. It is made up by a lower subunit (Tucle Volcanic Group; 0.8 Ma) composed by a series of andesitic to dacitic lavas and tuffs related to the uplift of the Tucle Horst, and a massive crystal-rich upper subunit (Tatio Ignimbrite Member; <1 Ma) with abundant plagioclase, biotite and horneblende. The ignimbrite has an heterogeneous composition and includes rhyolitic pumice clasts and mixed pumice.

Relevant units and rocks belonging to Miocene-Pleistocene ignimbrite of the volcanic San Bartolo Group were drilled by the exploration and production wells down to a depth of 1820 m (Healy, 1974). Common hydrothermal alteration minerals from cores and cuttings (Youngman, 1984) are montmorillonite, interlayered illite/montmorillonite, illite, chlorite and calcite; minor and rare minerals include hematite, anhydrite, albite-adularia and epidote. Pyrite was not observed in the drilled cores, probably due to the oxidation of H_2S in the fluid to SO_4^{2-} by Fe(III) in the Puripicar Ignimbrite. The Tatio Ignimbrite unit shows low intensity of alteration, that appears to be more pervasive at depth of 900–1000 m within the Puripicar and Salado volcanics.

The El Tatio geothermal field is about 30 km^2 in extent, but its major surface activity is restricted to an area of about 10 km^2. The latter includes geysers, hot pools, fumaroles, mudpots, as well as impressive sinter aprons, salt incrustations and growths of multicoloured microbes. Most geysers and spring vents lay out along NW-SE and NE-SW fractures. In the emitted gases, the major component is by far CO_2, followed by N_2, H_2S and CH_4 (Ellis, 1969). A magmatic intrusion at 5–7 km depth was suggested by Muñoz and Hamza (1993) in the area of El Tatio based on magnetotelluric soundings carried out by Schwarz *et al*. (1984), this intrusion being probably an andesitic-rhyolitic body at temperature of about 800°C and fairly rich in water. In addition, the hydrothermal convection was calculated to develop downwards to within 1 km from the magma intrusion or even nearer (Muñoz and Hamza, 1993).

Sampling and Analytical Procedures

Geysers, hot spring pools and mudpots were sampled in April 2002, and analyzed for major and trace element concentrations and isotopic compositions of hydrogen and oxygen of water, sulfur and oxygen of sulfate ions, carbon and oxygen of total dissolved carbonate and strontium in solution. Cold meteoric waters were also sampled in April 2002 (Rio Tucle), and cold spring and snow waters were kindly provided by the Earth Sciences Department of the Universidad Católica del Norte (Antofagasta). In addition to waters, the sulfur isotope composition of pyrite and molybdenite samples from the porphyry-copper Chuquicamata deposit in the Atacama desert was determined.

Temperature, pH, electrical conductivity and total alkalinity (titration method with methyl orange indicator) were measured in situ. Sodium, potassium, calcium and magnesium were determined by atomic absorption spectrometry following the procedures proposed by Bencini (1977); the relative accuracy of these methods is in the range of ±3 to ±5%. Chloride was analysed by Volhard's volumetric method and sulfate by turbidimetry/spectrophotometry with relative accuracies of ±7 to ±10% (APHA-AWWA-WEF, 1995). The concentrations of Al, B, Ba, Fe, Zn were measured by ICP-OES (ULTIMA 2 JOBIN-IVON instrument), and As, Co, Cr, Cs, Cu, Fe, Li, Mn, Mo, Pb, Rb, Tl, Zn by ICP-MS (X7 THERMO ELEMENTAL instrument). Quantification of As, Li, Mn and Sr was averaged from ICP-OES and ICP-MS results. For accuracy, precision, determination/quantification limits and strategy of the ICP-MS multi-element analytical method see Boschetti *et al*. (2001). Total I and Br in the water samples were determined by FI-ICP-MS (an ICP-MS PLASMAQUAD 3 VG ELEMENTAL instrument was coupled with a gradient pump GP-40 DIONEX and an automatic injection valve ERC iVALVE) using only 15 μl of sample and rising the system by a solution of 0.5% NH_3 solution Carlo Erba RPE; quantification limit and precision are 0.05 ± 0.03 μg/L for I and 7.0 ± 0.6 μg/L for Br (Boschetti, 2003).

The concentration of Si as SiO_2 was averaged by the ICP-OES and the spectrophotometric results. After filtration through 0.45 μm Millipore® and dilution in the field to prevent precipitation, water was reacted with

ammonium molybdate and measurements carried out with an accuracy of ±3–5%.

The δ^2H and δ^{18}O of waters were determined, respectively, by reaction of water with metallic Zn at 500°C (Kendall and Coplen, 1985) and by equilibrating CO_2 with water at 25°C (Epstein and Mayeda, 1953), then analysing H_2 and CO_2 in the mass-spectrometer. The results are relative to the V-SMOW standard. Duplicate preparations and analyses agreed within (1‰ for hydrogen and ±0.1‰ for oxygen). The tritium (^{3}H) measurements were carried out using the Cameron's (1967) method. The concentration is reported in tritium units (TU), that is the number of T atoms relative to 10^{18} H atoms. The analytical accuracy was within 1 TU.

Aliquots of waters were sampled for sulfur and oxygen isotopic analyses of dissolved sulfate. In the field, a spatula pit of calomel (Hg_2Cl_2) was added to all samples in order to stop the sulfate-reducing bacteria. In laboratory, the water samples were filtered through a 0.45 μm Millipore® filter. Aqueous sulfate was precipitated as barium sulfate after concentration by evaporation, and then reacted by the continuous-flow combustion technique to yield SO_2 for the mass-spectrometric sulfur isotope analysis basically following Geisemann *et al.* (1994) or CO for the mass-spectrometric oxygen isotope analysis according to Kornexl *et al.* (1999). The results are expressed in terms of δ^{34}S and δ^{18}O values, in per mill, relative to Canyon Diablo Troilite (CDT) standard for sulfur and V-SMOW standard for oxygen. Analyses have an uncertainty of ±0.2‰ for sulfur and ±0.4‰ for oxygen. Sulfate in the waters was concentrated by evaporation (Mizutani and Rafter, 1969) at 70°C and not by anion exchange because chloride is by far the major anion in the El Tatio hot waters and works as eluent. Only sulfate from cold spring (sample 9) and Rio Tucle (sample 15) were separated by anion exchange treatment using Dowex AG 1-8X, 50–100 mesh, chloride form resin as recommended by Nehring *et al.* (1977). Sulfur from metallic sulfides was extracted as SO_2 applying the same procedure used for the barium sulfate precipitates.

The δ^{13}C value of total dissolved carbonate was determined on barium carbonate prepared adding sodium hydroxide and barium chloride in the waters just after sampling in the field. The results are referred to PDB standard, and the analytical uncertainty is ±0.2‰.

Sr isotopic composition was determined in 1–3 g water evaporated to dryness and redissolved in 2.5 M HCl. Then, Sr was extracted from the hydrochloric solution by conventional cation exchange technique. The blank for the whole procedure was of 0.7 ng Sr. The ^{87}Sr/^{86}Sr ratio was measured by means of a VG Isomass 54E mass spectrometer, and normalized to a ^{86}Sr/^{88}Sr value of 0.1194 in natural strontium. Repeated analyses of NBS 987 $SrCO_3$ standard during the period of interest yielded an average ^{87}Sr/^{86}Sr ratio of 0.71024 ± 0.00002.

PHREEQCI software, version 2.8.0.0 (Parkhurst and Appelo, 1999), was adopted to compute aqueous speciation and fluid-mineral equilibria, using the "thermo.com.V8.R6" thermodynamic database (full LLNL database). Computed saturation indexes (SI) are approximate due to analytical and activity uncertainties, and for these reasons saturation is assumed to realize when SI = 0 ± 0.2.

Results and Discussion

The major and trace element composition of water in geysers, hot pools and mudpots (hereafter called as springs) are given in Tables 1 and 2, respectively. The isotopic compositions are reported in Table 3. The loca-

Table 1. Major element composition of hot pools, geysers and cold meteoric waters at El Tatio

Sample	Description	Sampling date	Temp. (°C)	pH (Twater)	Conductivity (mS/cm)	TDS (mg/l)	Ca^{2+} (mg/l)	Na^+ (mg/l)	Mg^{2+} (mg/l)	K^+ (mg/l)	Cl^- (mg/l)	tAlk (mg/l)	SO_4^{2-} (mg/l)	SiO_2 (mg/l)
1	pool	17-Apr-2002	73.6	6.01	22.9	12946	259	4338	0.43	501	7622	22.0	42.7	169
2	geyser	17-Apr-2002	73.5	6.39	21.7	13104	235	4322	0.64	477	7810	55.5	44.2	184
3	geyser	17-Apr-2002	77.2	7.23	22.4	12344	235	4211	0.31	538	7100	47.0	42.4	190
4	pool	17-Apr-2002	74.4	7.14	20.5	13241	231	4404	0.22	542	7810	37.2	43.1	188
5	geyser	17-Apr-2002	73.4	7.33	21.9	13270	227	4345	0.75	519	7899	55.5	42.9	205
6	pool	17-Apr-2002	74.8	6.97	22.0	13462	242	4459	0.64	595	7891	60.4	42.5	198
7	pool	17-Apr-2002	67.0	6.57	21.6	11962	219	4035	1.51	469	7011	40.9	43.6	159
8	geyser	17-Apr-2002	70.8	7.61	19.0	10555	221	3591	0.76	320	6213	80.5	38.8	128
9	cold spring	17-Apr-2002	9.6	7.77	0.14	98	4.8	20.5	1.73	3.6	18	25.6	15.4	21
10	geyser	18-Apr-2002	77.6	7.22	20.5	10146	259	3463	0.89	170	6035	55.5	52.5	135
11	pool	18-Apr-2002	49.8	6.45	16.4	10516	242	3534	1.64	195	6301	36.0	51.5	169
13	geyser	18-Apr-2002	76.4	7.07	0.61	444	29	66.4	7.7	15.6	8.8	62.2	179	105
14	mudpot	18-Apr-2002	76.4	5.73	0.89	405	34	47.1	12.2	13.9	11.9	27.5	273	—
15	Tucle stream	18-Apr-2002	14.8	8.22	0.59	276	33	23.1	15.7	9.4	8.4	119	87.5	39

tAlk = total alkalinity, where data are expressed as mg/l of HCO_3; — = not analysed; TDS (Total Dissolved Solids) = 0.5(tAlk) + Ca^{2+} + Na^+ + Mg^{2+} + K^+ + Cl^- + SO_4^{2-} + 1.02(SiO_2) (modified from APHA-AWWA-WEF, 1995).*

Table 2. Minor and trace element composition µg/l of hot pools, geysers and meteoric waters at El Tatiomg/l

Sample	Description	Al (µg/l)	As (µg/l)	B (µg/l)	Ba (µg/l)	Br (µg/l)	Co (µg/l)	Cr (µg/l)	Cs (µg/l)	Cu (µg/l)	Fe (µg/l)	I (µg/l)	Li (µg/l)	Mn (µg/l)	Mo (µg/l)	Ni (µg/l)	Rb (µg/l)	Sr (µg/l)	Tl (µg/l)	Zn (µg/l)
1	pool	8.6	34950	155320	70	7957	1.5	4.3	13380	9.8	<3	569	33460	76	41.5	11.5	4449	4153	21	119
2	geyser	11	39330	163880	161	8144	1.4	3.8	13760	17	<3	783	34270	340	44.8	15.2	4946	3977	29	61
3	geyser	7.7	36760	156110	153	7823	1.4	2.7	13480	11	5	549	33420	241	45.5	15.4	4808	3745	26	59
4	pool	6.3	35790	157220	236	7798	1.7	2.5	13880	31	<3	—	33990	168	46.7	14.9	4964	3781	30	86
5	geyser	8.9	36560	156810	168	7551	1.4	2.0	12960	15	<3	280	32600	343	44.9	16.2	4915	3740	29	51
6	pool	7.4	37550	156860	242	7201	3.6	10.3	13470	17	6	253	32490	338	43.4	16.1	4604	3625	50	101
7	pool	4.7	35750	147750	135	6902	1.7	—	12530	9.5	3	—	30450	336	44.4	11.9	4438	3609	24	96
8	geyser	3.7	28790	128800	77	2929	1.0	—	5432	8.7	<3	225	12840	336	22.9	8.9	1464	3623	—	1
9	cold spring	12	17	95	4	14	0.027	0.3	10	0.61	4	—	11	0.4	0.35	0.2	9	42	<0.02	9
10	geyser	17	29830	128400	66	6071	1.0	—	10700	8	<3	—	23110	109	44.8	10.4	1978	3734	—	53
11	pool	5.9	28980	129980	80	6070	1.6	—	11090	39	<3	—	24040	114	45.6	12.6	1955	3757	—	441
13	geyser	14	27	2590	76	28	0.093	0.03	27	0.58	3	31	37	39	2.6	0.7	44	220	<0.02	6
15	Tucle stream	2.8	21	319	24	22	0.140	0.2	2		54	16	13	2.9	1.3	0.7	24	170	<0.02	3

— = *not analysed.*

tion of the sampling sites is shown in Fig. 1. Springs 1 to 7 are located in the northern part of the main thermal area along a SW-NE trending fault, springs 8, 10 and 11 close to the western border of the field, and springs 13 to 14 along the south-western margin.

Major element composition

The measured concentration data are plotted in the trilinear diagrams of Fig. 2, together with those from other studies (Giggenbach, 1978 and references therein). The chloride waters fall in the maturity field as defined by Giggenbach (1988), steam-heated waters are of sulfate or bicarbonate type, and local cold meteoric waters are bicarbonate. All waters are rich in sodium relative to the other major cations. As shown by the plot, total alkalinity, potassium and chloride define trends which distinguish springs fed by three different reservoirs, A, B and C, as already thought by Giggenbach (1978). Deviations towards the potassium corner may be explained by a temperature-dependent exchange of Na and K between the fluids and alkali feldspars (Youngman, 1984; Giggenbach, 1988). It is remarkable that springs 10 and 11 from this study should issue from reservoir B.

The maturity of the chloride waters (our samples and the historical ones) is confirmed by the Giggenbach's (1988) diagram of Fig. 3, where the cations in solution appear to be in equilibrium with primary and secondary minerals in the aquifers. Data points fit the equilibrium weirbox curve (that considers the chemical effects due to single-step separation of vapor from the fluid), and once again identify two possible chloride-water reservoirs at about 270°C (point A) and 170°C (point B). Sulfate steam-heated waters and meteoric waters are totally immature, and appear to be devoid of magnesium. Deviations from the Na-K-Mg equilibrium curve can be interpreted as due to mixing with near-surface water (see dashed lines in Fig. 3).

Sodium-chloride hot waters

Sodium and chloride are the dominant ions in geysers and hot pools, with concentrations of 3591 to 4459 mg/l and 6035 to 7899 mg/l, respectively. These high values are normally observed in hot springs fed by fluids that rise rapidly from the reservoir, and thus delineate the upflow zone of the geothermal system. Chloride may primarily derive from HCl degassing from a magma chamber located along the flow path of the water that feeds the geothermal reservoir or lying just beneath the El Tatio geothermal system. In this case, fluid-rock interaction should be a secondary source of chloride. In fact, the Na/Cl by weight ratio of 215 in fresh dacite of the Central Volcanic Zone of Andes in northern Chile (Matthews *et al.*, 1994) is much higher than the average one of 0.567 in the El Tatio hot springs. The main source of sodium in

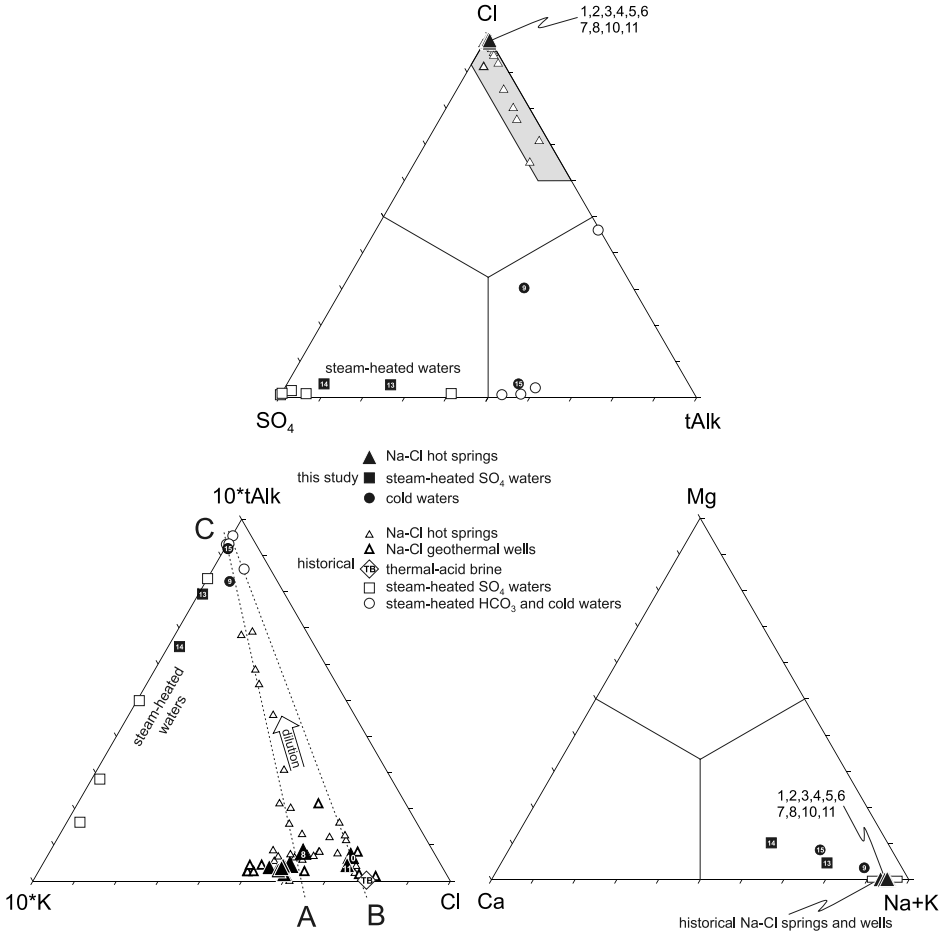

Fig. 2. Major anion composition of our samples (filled symbols) and historical water samples from literature (open symbols; see text for references). Hot springs (triangles), well waters (edged triangles), steam-heated SO_4 waters (squares), steam-heated HCO_3 waters and cold meteoric waters (circles). The El Tatio thermal acid brine (TB) is from Giggenbach (1978). The grey box in the SO_4-Cl-tAlk diagram represents the compositional field expected for mature (sodium-chloride) hot springs (Giggenbach, 1988). Numbers refer to the present study samples (see Table 1).

the fluids can be the leaching of host rocks, especially of dacites and rhyolites (e.g., Ellis and Mahon, 1967). Potassium is also a major cation (170 to 595 mg/l). Its concentrations do not relate proportionally with sodium, that is the Na/K ratio in the water is likely controlled by temperature (inverse correlation). Based on the lower Na/K by weight ratios (<15), water of springs 1 to 8 can be associated with a more direct feeding from the reservoir, whereas water of springs 10 and 11 (Na/K > 15) is probably provided by lateral flows and then may undergone near-surface reactions and conductive cooling (Nicholson, 1993).

Calcium (221 to 259 mg/l) and magnesium (0.2 to 1.7 mg/l) concentrations are controlled by a variety of factors, that include retrograde solubility of minerals and P_{CO2} for calcium and incorporation into alteration clay minerals for magnesium. The higher Ca/Mg by weight ratios in springs 1 to 8 relative to springs 10 and 11 agree with the hydrological interpretation based on the Na/K ratios.

Total alkalinity (22 to 81 mg/l) and sulfate (39 to 53 mg/l) are minor components in solution. As calculated applying the PHREEQCI software, the contribution of the polyprotic acids to the non-carbonate alkalinity is quite high (>51%), and principally due to silica, boric acid and arsenate. The concentration of sulfate is low, as usually observed in deep geothermal fluids. Probably, some sulfate derives from the oxidation of H_2S (up to 12 mg/l in the Na-Cl springs; Ellis, 1969). Unfortunately, we have not measured H_2S, total sulfur and Eh in the fluids.

Silicic acid (135 to 205 mg/l as SiO_2) derives from silicate dissolution in the depth. Its concentration values show a rough negative correlation with the Na/K concentration ratios, in agreement with the relations between the

two parameters and temperature. It correlates positively with chloride, suggesting that the highest is the chloride content in the spring, the most direct is the supply from the main geothermal reservoir in the depth.

Hydrogen ion concentration

The pH value of the fluid in the El Tatio main geothermal reservoir hosted within the Puripicar Ignimbrite should be controlled basically by equilibria with Na-K-Ca minerals as well as by the carbon dioxide partial pressure in the fluid. It can be computed applying the Chiodini *et al.*'s (1991) equation to waters from drilled wells 1 (211°C), 7 (250°C) and 11 (240°C) which should tap the main aquifer (Youngman, 1984). Maximum temperatures in the wells before discharge were estimated to be 211, 250 and 240°C. The mentioned equation is:

$$pH = 1.757 - 0.822 \log \sum eq + 1846/T - 0.0171 \log P_{CO2}$$

where T in °K, P_{CO2} = 1.26 to 1.40 bar depending on well, $\sum eq = \sum |z_i| m_i$ = salinity of the well water with z_i and m_i being the ionic charge and the molality of the i-th ion species (major cations and anions). The chemical data were taken from Youngman (1984) and corrected for the evaporation effects.

The resulting average pH value is 5.79 ± 0.15, that matches very well with that of 5.76 reported by Youngman (1984). It may be of interest that the pH value of 5.67 computed for well 7 (showing the highest enthalpy) from the above equation is in good agreement with that of 5.50 calculated using the PHREEQCI software.

Sodium-sulfate hot waters

These waters are located along the southwestern margin of the field. Their sulfate concentration (179 and 273 mg/l) is higher than the one of the local surface waters (15.4 and 87.5 mg/l). This is the result of near-surface steam condensation and oxidation of carried H_2S. The pH value of 5.6 in mudpot 14 denotes a substantial neutralization of acidity basically by mineral-fluid reactions. In the geyser 13, the rising gases interact with shallow water, the latter being provided by the Rio Tucle. The much higher magnesium content in these sulfate waters agrees with near-surface low-temperature reactions leaching local rocks (spring 14) or dilution by surface water rich in magnesium (spring 13).

Local surface waters

A sodium-bicarbonate dilute cold spring water with TDS of about 98 mg/l, and a calcium-bicarbonate water sample with TDS of about 276 mg/l from the Rio Tucle were analysed. In both cases there is no geothermal influence.

Trace element composition

Chloride springs 1, 2, 3, 4, 5, 6, and 7 in the central part of the field are characterized by high and nearly uniform concentrations of cesium (12.53 to 13.88 mg/l), arsenic (34.95 to 39.33 mg/l), lithium (30.45 to 34.27 mg/l), boron (147.75 to 163.88 mg/l) and bromine (6.90 to 8.14 mg/l). Chloride springs 8, 10 and 11 from the western end of the field show considerably lower concentration of cesium (5.43 to 11.09 mg/l), arsenic (28.79 to 29.83 mg/l), lithium (12.84 to 24.04 mg/l), boron (128.4 to 130.0 mg/l) and bromine (2.93 to 6.07 mg/l). Sulfate spring 13 appears to be largely diluted by Rio Tucle, and its trace element concentrations are on the whole comparable, even if higher, with those of the stream. The rubidium and strontium concentrations follow those of potassium and calcium, respectively. Iodine concentrations in chloride waters range between 225 and 783 μg/l, and positively correlate with bromine. There is a low concentration of all base metals. Finally, the high levels of arsenic in solution can be considered as normal in this volcanic district of the Andes, and are possibly related to the leaching of metal sulfides in the rocks (23 to 36 ppm in the unaltered Puripicar-Salado ignimbrite; Youngman, 1984). At the Eh values calculated using redox pairs S(–2)/S(+6) from literature data (Youngman, 1984 and references therein) on wells (mean –0.254 V) and springs (–0.101 V), $H_2AsO_4^-$ and $HAsO_4^{2-}$ are the predominant As species in solution.

The relatively high concentration values of some transition elements like Mn, Mo and Ni may be related to effects upon the solubility of these metals due to the high salinity and the low pH of the fluids.

Molecular ratios

In the chloride springs, the Cl:B ratio shows a narrow range of variation. This suggests a common feeding body of hot water and an ascending path along one supply fissure or through chemically very homogeneous rocks. The slight deviation of some analyses may be due to local contamination by shallow water. The Na:K and Na:Li ratios have a similar behavior, displaying groups of values as if thermally distinct aquifers are involved. The Na-Li geothermometer (Kharaka *et al.*, 1982) yields by 16 to 84°C higher estimates; probably, the Na:Li ratio is somehow affected by low-temperature subsurface adsorption of lithium onto clays or alteration products, particularly in the springs 10 and 11 which show comparatively high Na/Li ratios. These springs may be fed significantly by lateral flow, where lithium is partially removed from the solution. This interpretation is supported by the Li-Mg geothermometer (Kharaka and Mariner, 1989), which also yields similar or higher estimates. Similarly, the Na/Ca ratios display three groups of values, corresponding to

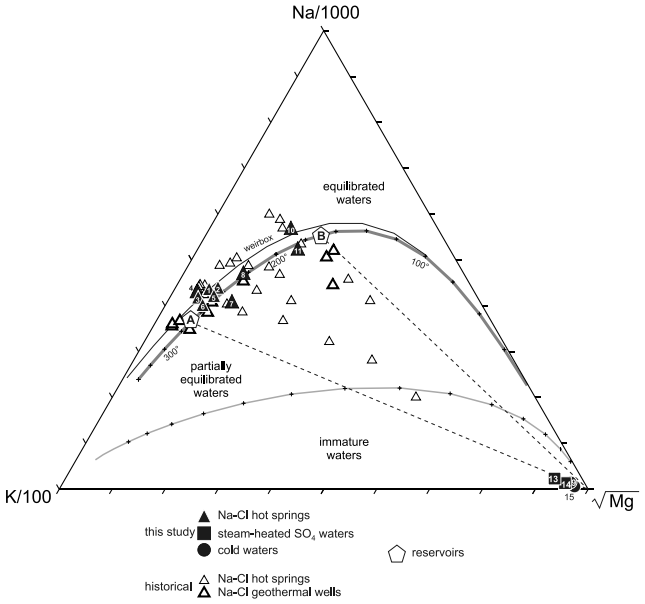

Fig. 3. Trilinear diagram showing the relative concentrations of Na, K and Mg in our hot and cold waters (filled symbols) and in historical hot waters (open symbols; see text for references) at El Tatio, compared with the non-equilibrium to equilibrium fields as discussed by Giggenbach (1988). The weirbox curve considers the effects due to single-step loss of steam. A and B identify the main and the secondary chloride geothermal reservoirs envisaged at El Tatio (see Giggenbach, 1978). Numbers refer to the present study samples (see Table 1)

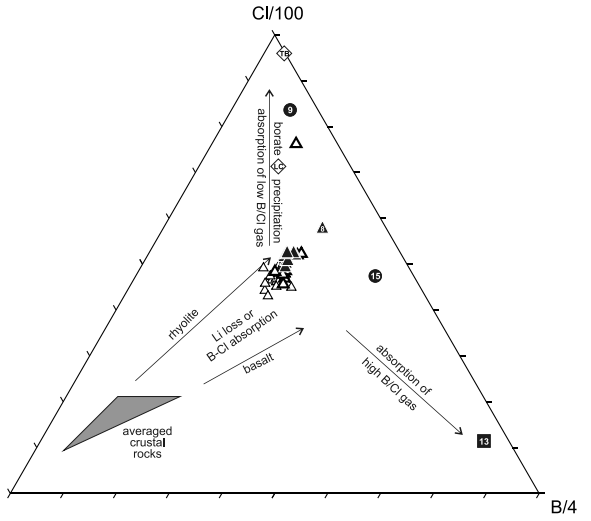

Fig. 4. Cl-Li-B ternary plot, where our data (Na-Cl hot springs = filled triangle; Na-SO_4-hot spring = filled square; cold meteoric waters = filled circles) are compared with previous ones from literature (see text for references), the latter dealing with hot springs and wells and cold waters (corresponding symbols are open). Coherent data on these elements in rocks from the Central Volcanic Zone (CVZ) of Andes are lacking, and therefore data on "average crustal rock" (Taylor, 1964) are used in the plot. TB = El Tatio Drive. LC = Laguna Colorada.

distinct Na-K-Ca thermometric estimates. However, this geothermometer is not recommended, as the molar [$Ca^{1/2}$/Na] ratios in the springs are much less than unit (Fournier and Truesdell, 1973). The Cl to Br, As and Cs ratios are similar in the studied springs, thus corroborating a common source reservoir. Exception is spring 8 which is depleted in trace elements, probably because of mixing with shallow water that appears to be very poor in Br, As and Cs relative to Cl.

In the sulfate springs, the Cl to B, Br and I ratios are lower, in agreement with the higher proportion of boric, hydrobromic and hydriodic acids relative to hydrochloric acid in the steam leaving the geothermal reservoir. As expected, they are lower than those observed in the local meteoric waters. The Cl:As ratio is higher than in chloride waters, but it is lower than in meteoric water. Finally, the ratios involving cations are influenced by the widespread disequilibrium of these sulfate waters relative to host rocks.

In Fig. 4 the evolutions of related to hydrothermalism elements like Li and B are depicted, starting from the isochemical dissolution of an averaged andesitic-rhyolitic rock, followed by exchange with secondary minerals or interaction with gases. Our data are compared with those of Cusicanqui *et al*. (1975) and Giggenbach (1978) dealing with both hot springs and exploration wells. The El Tatio acid brine has a B/Cl by weight ratio close to zero (Giggenbach, 1978), which is typical of high chloride volcanic acid waters (see figure 10 in Giggenbach and Soto, 1992). On the other hand, the Laguna Colorada basic brine (pH = 8.2; 20 km east of El Tatio; Giggenbach, 1978) lies nearly on the same trend, and may be interpreted as being originally a geothermal water that probably lost boron by precipitation of ulexite (Chong *et al*., 2000).

More on the aqueous I/Cl and Br/Cl ratios in the El Tatio waters

Iodine in geothermal waters and fumaroles from volcanic andesitic setting basically derives from the subducted slab sediments (e.g., Fehn and Snyder, 2003). Its concentration in the fluids depends on several factors and processes (Honda *et al*., 1966), included the position of the geothermal reservoir relative to the accretion prism, the proportion of continental to oceanic crust in the slab and the working heat fluxes, as well as precipitation/dissolution of sublimates, evaporation and dilution during the fluid uprising. The same source and processes are expected to control the bromine and chlorine concentrations in the fluids.

The data from hot springs of El Tatio are compared in Fig. 5 with those available for other geothermal and volcanic fluids in Chile and throughout the world, as well as for meteoric waters. First of all, the main feature is the similar chemical composition of I and Br in the chloride-waters from the El Tatio and the Sol de Mañana (Bolivia) geothermal fields, both of them being active and close. The latter fit mixing trends with shallow meteoric water for both I and Br, the agreement being much better for Br, whereas some springs show I concentration values lower than expected. Also the geothermal waters from Peruvian fields distribute along dilution lines with meteoric water; in these waters, the I/Cl ratio is high and matches the maximum ratio measured in pore fluids in Peru margin sediments (Martin *et al*., 1993). Another remarkable feature shown by the I/Cl and Br/Cl ratios in the fluids from the above two geothermal fields is that they are considerably lower than those observed in volcanic fluids from the Central American Volcanic Arc (CAVA), thus suggesting a higher proportion of continental crust (with minor I and Br) in the subducted slab at about 22°S latitude. However, an alternative explanation for the scattering of the I/Cl and Br/Cl ratios in the Andean geothermal fluids may be related to variable contributions of andesitic waters to the feeding reservoirs. Assuming that the halides under question almost completely derive from the slab and applying the chemical ratios measured in our chloride-richest springs (1 to 6 samples; I/Cl ≈ 6.4×10^{-5}; Br/Cl ≈ 1.0×10^{-3}), mean values of about 1 to 1.3 ppm I and 15 to 20 ppm Br are calculated for the hypothetic magmatic-andesitic (15,000 to 20,000 ppm Cl) water at El Tatio. With respect to the CAVA geothermal fluids (Snyder and Fehn, 2002), these concentration values are comparable with those observed in Nicaragua and Costa Rica geothermal fluids, but considerably lower than observed in El Salvador, probably accounting for the lower distance along the arc of the geothermal fields in the latter country.

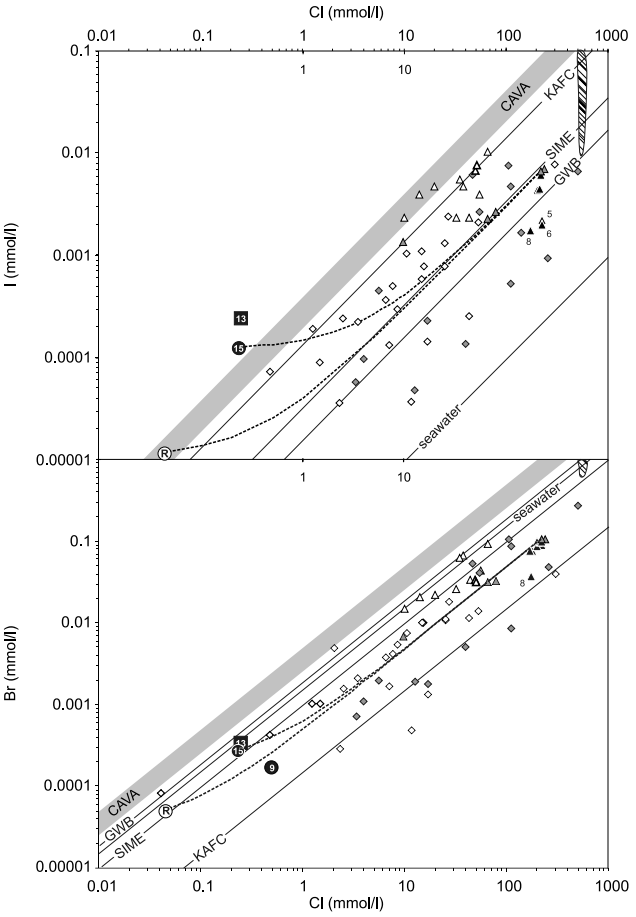

Fig. 5. I-Br-Cl relations of hot and cold waters from El Tatio and other geothermal and volcanic systems throughout the world. Geothermal systems: edged triangles = Empexa, Bolivia (Scandiffio and Cassis, 1992); open triangles = Tutupaca and Chappalca, Peru (Scandiffio et al., 1992); grey triangles = Sol de Mañana, Bolivia (Scandiffio and Alvarez, 1992); CAVA = fitting of data on geothermal waters from the Central American Volcanic Arc in Costa Rica, Nicaragua and El Salvador (Snyder and Fehn, 2002); GWB = fitting of data on hot waters from Broadlands, Taupo Volcanic Zone, New Zealand (Fehn and Snyder, 2003). Volcanic systems: KAFC = fitting of data on Kuril Arc fumarolic condensates (Taran et al., 1995); SIME = Br and I to Cl ratios estimated for the Satsuma-Iwojima magmatic end member (Snyder et al., 2002). Dashed band: pore fluids in Peru margin sediments (Martin et al., 1993). Open circle R = global rain water value (Yuita, 1994).

Li-Rb-Cs relationships

The relative proportions of the cations under question in the hot and cold waters are shown in the ternary diagram of Fig. 6, compared also to the composition of Late Cenozoic calc-alkaline lavas of the Central Volcanic Zone (CVZ) of Andes between 28° to 16° latitude (Déruelle, 1982; Lindsay *et al*., 2001). In the sodium-chloride springs and wells from our study and from previous ones, the Li/Cs ratios preserves nearly identical as in the host dacites, whereas the Rb proportion is lowered probably due to uptake by illite, the latter mineral being abundant in the high temperature alteration levels of drilled cores at El Tatio (Youngman, 1984). The rock composition is approached by the steam-heated spring, as well as by the low-pH brine found at depth beneath El Tatio field (see introduction section). Probably, these waters react with heavily altered vulcanites and their initial acidity is not completely neutralized, as concluded by Risacher *et al*. (2002) for the Gorbea and Ignorado acid salars in northern Chile.

Samples from the Laguna Colorada brine (Giggenbach, 1978; Scandiffio *et al*., 1992) are plotted as comparison in Fig. 6. Their trend in the plot may be

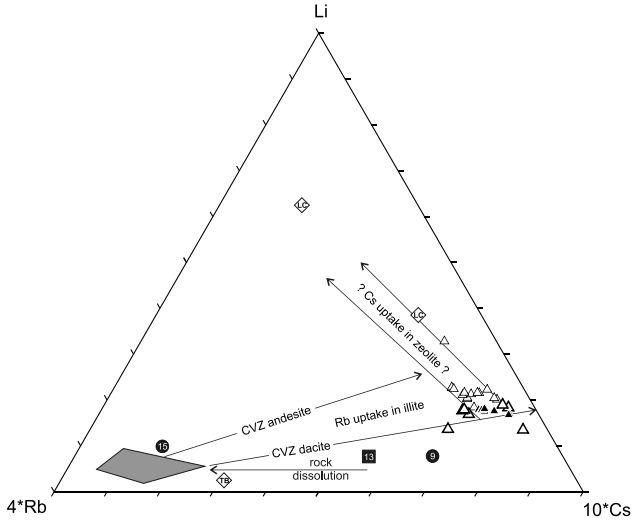

Fig. 6. Li-Rb-Cs trilinear diagram. Chemical data, symbols and abbreviations as in Fig. 4. The shaded polygon identifies the calc-alkaline lavas from CVZ (see text for references). Rock dissolution denotes a non-equilibrium isochemical process.

explained with a progressive enrichment in Li (see Ericksen *et al.*, 1978) rather than with a Cs uptake by zeolites (analcime, wairakite). At El Tatio, zeolites are rare as hydrothermal alteration products (Youngman, 1984) but they should be very rich in Cs as found elsewhere by Goguel (1983) in wairakite (4500 ppm Cs).

Thermometric estimates

The silica concentration in the chloride waters is fairly uniform within the range 160 to 205 mg/l. Applying the quartz geothermometer (see Nicholson, 1993 for a review), calculated temperatures are in the range 145 to 170°C (adiabatic cooling of the fluid by steam loss after leaving the reservoir). If no steam loss is assumed, the estimates are 30–40°C higher. The latter are in turn up to about 50°C lower than the Na/K ones estimated applying the Giggenbach's (1988) thermometer. In addition, springs 8, 10 and 11 do not follow the thermometric trend visualized in Fig. 3. All these thermometric features concur to support that the original silica concentration in the fluid was affected by boiling and/or dilution.

New Na/K (Verma and Santoyo, 1997; Can, 2002) and SiO_2 (Verma, 2001) geothermometers were recently published in current literature. In Fig. 7, the Na/K thermometric estimates from new and old (Giggenbach, 1988) equations are compared with those from the Verma's (2001) quartz thermometer. The estimates refer to water samples from the exploratory wells of El Tatio (Cusicanqui *et al.*, 1975; Giggenbach, 1978), after correction of the silica concentration data by calculating the steam fraction lost due to boiling during the ascension

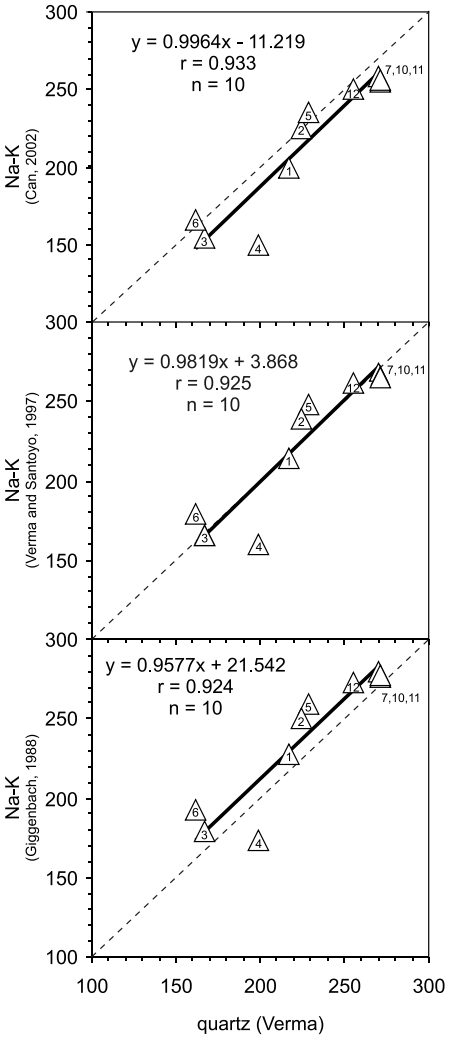

Fig. 7. Comparison of the results obtained from the old (Giggenbach, 1988) and recent (Verma and Santoyo, 1997; Can, 2002) Na/K geothermometers with those from the new SiO_2 geothermometer (Verma, 2001), applied to the geothermal well waters analysed by Cusicanqui et al. (1975) and Giggenbach (1978). The best fitting to the 1:1 dashed line is obtained applying the Verma and Santoyo's (1997) Na/K thermometer. The wells are numbered as in Cusicanqui et al. (1975).

(e.g., Fournier, 1981). The best fitting with respect to the equivalence line is shown by the Verma and Santoyo's (1997) Na/K thermometer, which yields a maximum temperature of 268°C when compared to the value of 271°C from the silica thermometer. The mean temperature of 270°C from wells fed by the main reservoir (wells 1, 2, 5 7, 10, 11, 12) is 10°C higher than the value reported by Giggenbach (1978). The Na/K temperatures from wells likely tapping the shallower reservoir B (wells 3, 4, 6; Youngman, 1984) average 172°C.

When applied to our chloride springs, the Verma and

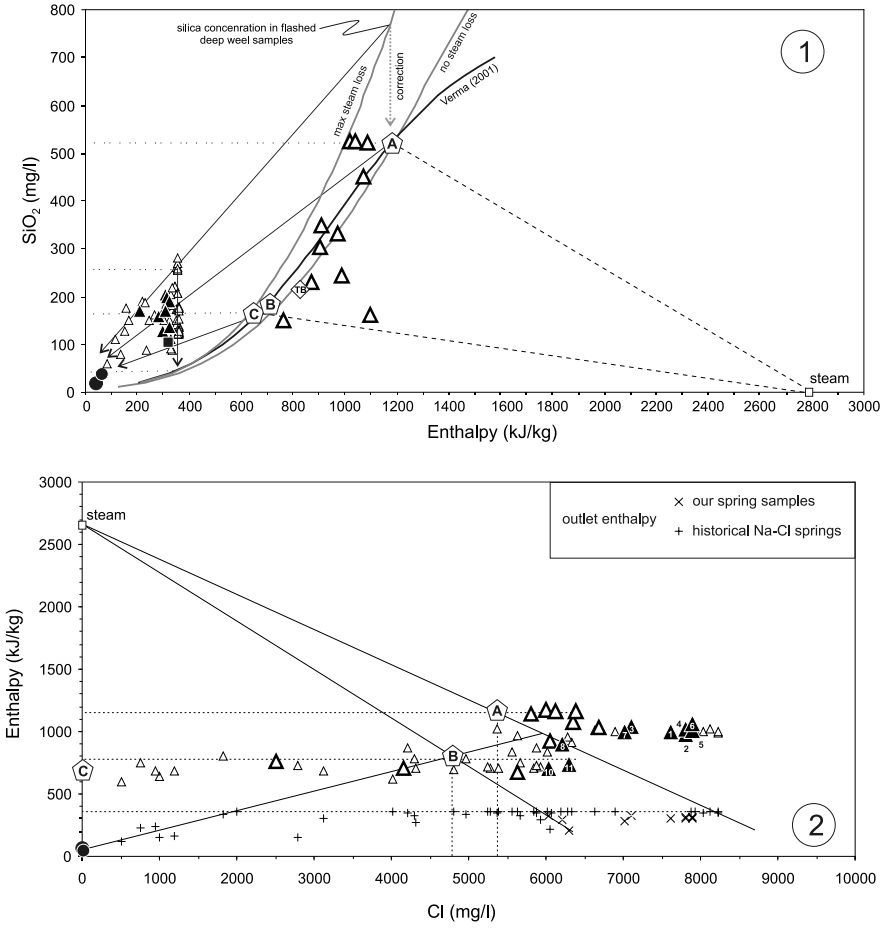

Fig. 8. SiO_2-enthalpy (plot 1) and Cl-enthalpy (plot 2) diagrams. In plot (1) the quartz solubility curve of Verma (2001) is also shown in addition to those reported in Nicholson (1993) for no steam loss and maximum steam loss solubility. Our (filled symbols) and previous (open symbols) data on hot springs (triangles) and wells (edged triangles) are plotted, along with data on meteoric cold waters (filled circles). A silica concentration of 750 mg/l is estimated for flashed water A at 270°C, that reduces to 524 mg/l after correction for the loss of steam (i.e., in the reservoir A before flashing). The reservoir B is fed by reservoir A, then cools down to about 170°C and re-equilibrates with mineral phases. The reservoir C (about 160°C and 160 mg/l SiO_2) may be fed partially by fluids from the reservoir B rather than from the reservoir A, as also suggested by Giggenbach (1978). In plot (2) all studied hot and cold waters at El Tatio (this work; Youngman, 1984 and references therein) are reported, with the enthalpy values calculated at the outlet temperature and at the chemical Na/K and SiO_2 temperatures. The main and subordinate reservoirs are shown, as well as some possible binary mixing trends.

Santoyo's (1997) Na/K equation yields temperatures of 228 to 245°C for springs 1 to 7, 211°C for spring 8, and 168 to 175°C for springs 10 and 11. These estimates are considerably lower than the main reservoir temperature, possibly due to a variety of processes including re-equilibration before discharge.

Enthalpy-silica and enthalpy-chloride models

Enthalpy-silica and enthalpy-chloride models are shown in Fig. 8. They allow to estimate the silica and chloride contents of the reservoir fluids before boiling and mixing/dilution processes. In the main aquifer A, at 270°C, in the Puripicar Ignimbrite unit, the silica and chloride concentrations are estimated to be close to 520 mg/l and 5,400 mg/l, respectively. In the secondary aquifer B, at 170°C, in the Tucle Dacite unit, the silica and chloride contents should approach 250 mg/l and 4800 mg/l, respectively. Finally, a silica content of 180 mg/l is inferred for the bicarbonate aquifer C, at 160°C (and 0 mg/l chloride and 250 mg/l bicarbonate; Youngman, 1984). Possibly, the reservoir C derives from the condensation of gas and steam evolved from the reservoir B, rather than directly from the reservoir A as interpreted by Giggenbach (1978). Relevant in this context is the stratigraphic re-

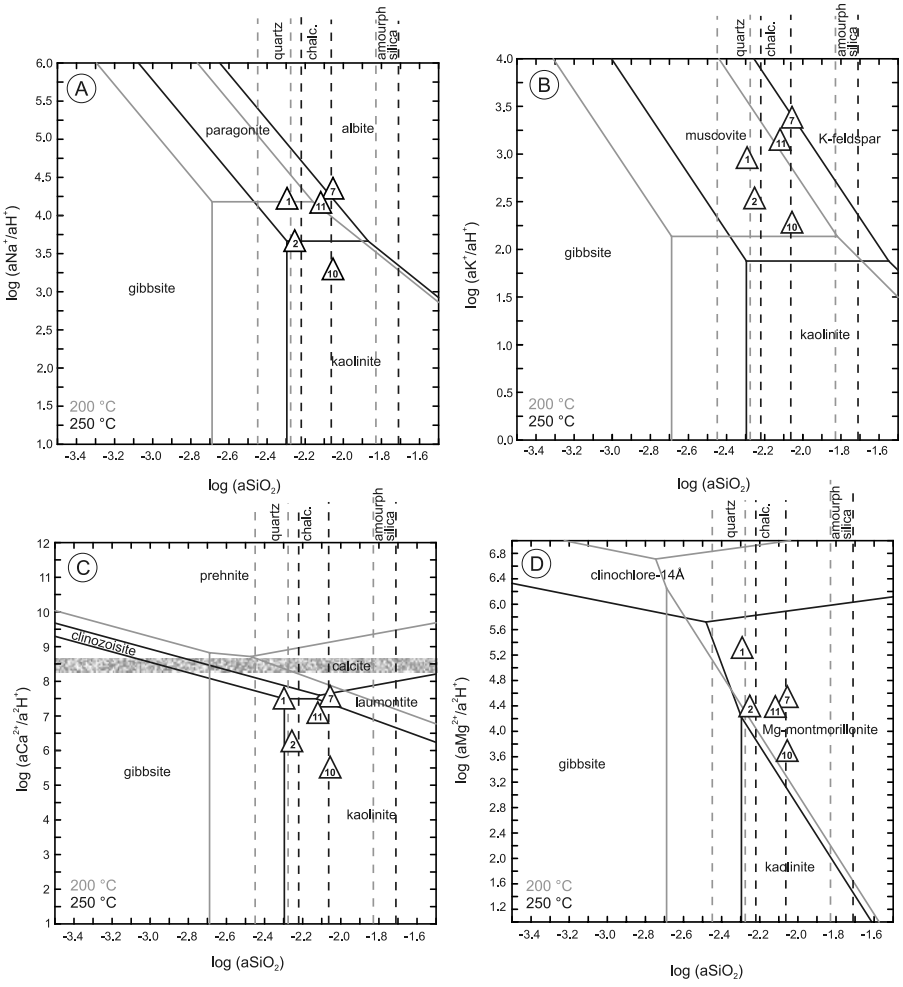

Fig. 9. Activity plots for the systems (A) Na_2O-Al_2O_3-SiO_2-H_2O, (B) K_2O-Al_2O_3-SiO_2-H_2O, (C) CaO-Al_2O_3-SiO_2-H_2O and (D) MgO-Al_2O_3-SiO_2-H_2O, at 200–250°C and corresponding water saturation pressure, and their application to selected geothermal well waters from El Tatio (see text for details and references). The grey band in diagram C delimits the solubility of calcite, as computed at calculated PCO_2 values of 0.022 to 0.153 bar. The "thermo.com.V8.R6" thermodynamic database (full LLNL database) was used for computation.

construction by which the Tucle Dacite unit (reservoir B) penetrates the Tatio ignimbrite unit (reservoir C) in the subsoil of El Tatio (De Silva, 1989).

Fluid-mineral equilibria

Activity diagrams are powerful graphical tools depicting the stability of solid phases with respect to the composition of the coexisting solution, while temperature and pressure are kept constant and solid assemblages are effectively presents in the geological environment.

The diagrams shown in Figs. 9 and 10 refer to El Tatio geothermal well waters from Ellis (1969; wells 1, 2, 7, 10, 11), with quartz adiabatic temperatures in the range 200 to 250°C, and possibly related to the main reservoir. Pressure was taken to be 15.5 bars at 200°C and 39.9 bars at 250°C, which correspond to the coexistence of vapour and liquid in a liquid-dominated reservoir. Activity diagram computation was performed after correction due to loss of steam of the chemical data on well fluids, and using the "thermo.com.V8.R6" thermodynamic database (full LLNL database) for Figs. 9 and 10A, and the "data0.3245r46" thermodynamic database (compacted LLNL database) for Fig. 10B. Details on databases can be found in Bethke (2002).

The activity plots for the systems Na_2O-Al_2O_3-SiO_2-H_2O, K_2O-Al_2O_3-SiO_2-H_2O, CaO-Al_2O_3-SiO_2-H_2O, and MgO-Al_2O_3-SiO_2-H_2O are shown in Figs. 9A to 9D. It appears that Na^+ activity is controlled by paragonite and/or albite, K^+ by muscovite and/or K-feldspar (adularia), Ca^{2+} by laumontite and/or clinozoisite, and Mg^{2+} by Mg-montmorillonite. According to Reed (1997), when we have to deal with a multicomponent system, the activity

plots cannot adequately account for the effects of coupled mineral equilibria, involving minerals and fluid components that are not represented on the diagrams. Thus, Ca^{2+} could be controlled by additional phases like calcite or anhydrite/gypsum. In the wells under question, the fluids are undersatured with respect to both calcite ($-2.9 < SI < -0.9$) and anhydrite ($-4.0 < SI < -2.2$); in spite of boiling at depth, the Na-Cl springs of El Tatio preserve the undersaturation state with respect to anhydrite, but in some cases they become saturated to oversatured with respect to calcite. According to the abundant calcite found in the exploration wells (Youngman, 1984), CO_2 content in the past fluids should have been higher than nowadays (Cusicanqui *et al*., 1975). Further uncertainties deal with (1) the presence of laumontite in the reservoir as computed at 250°C, even if laumontite should be stable below 250°C, and wairakite should form at higher temperature, and (2) the role of mixed layer alteration clay minerals (illite/montmorillonite), whose stability thermodynamic data are lacking. In Fig. 10, the activity diagrams describe the system $MgO\text{-}K_2O\text{-}Al_2O_3\text{-}SiO_2\text{-}H_2O$, when temperature raises up to 270°C, the maximum temperature estimated for the main reservoir, and were constructed imposing saturation with respect to quartz. In fact, these fluids appear to be saturated with respect to chalcedony ($-0.09 < SI < 0.07$) and then oversaturated with respect to quartz ($0.08 < SI < 0.23$) (Fig. 9). The latter was found in the drilled cores as vug filling and silicifications (Youngman, 1984), justifying the use of quartz geothermometer (see section on thermometric estimates). In Fig. 10A, the data plot into the Mg-montmorillonite field, as expected if smectite is the prevailing Mg-mineral in equilibrium with the fluids. Changing the database (Fig. 10B), water samples fall into or point to the illite stability field. These results are in keeping with the presence of interlayered illite/montmorillonite clays as found in altered rocks by Youngman (1984).

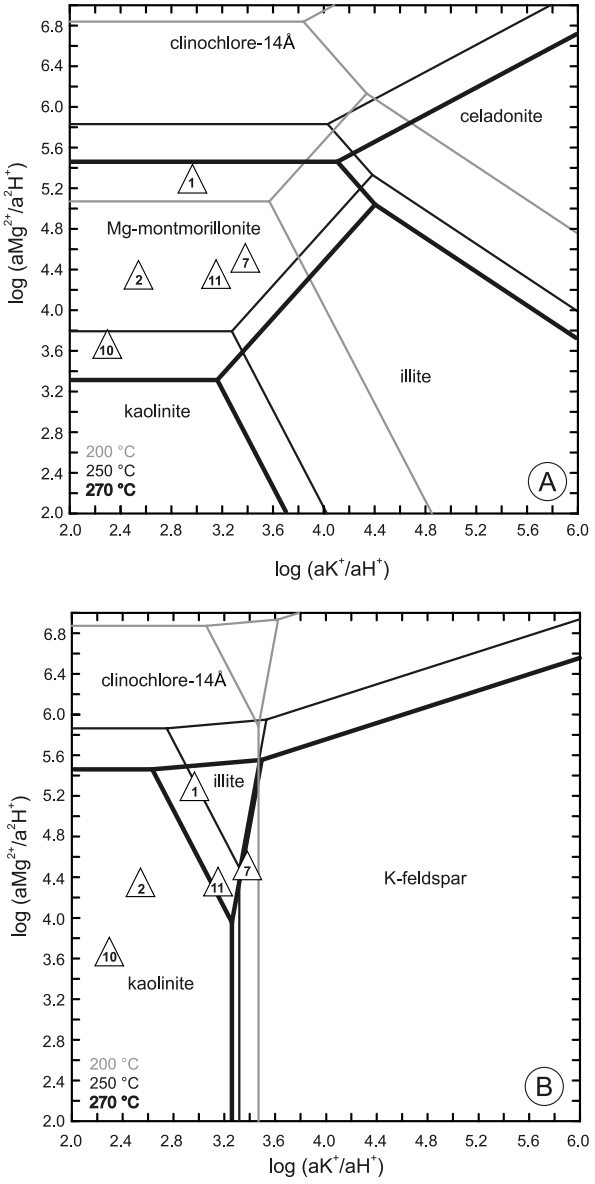

Fig. 10. Activity plots for the system $MgO\text{-}K_2O\text{-}Al_2O_3\text{-}SiO_2\text{-}H_2O$ at 200–250–270°C and corresponding water saturation pressure, and their application to selected geothermal well waters from El Tatio (see text for details and references). Diagrams A and B were constructed by means of the "thermo.com.V8.R6" (full LLNL database) and "data0.3245r46" (compacted LLNL database; Bethke, 2002) databases, respectively.

Isotopic compositions

Isotopic analyses were performed on water ($^2H/^1H$, ^3H, $^{18}O/^{16}O$), dissolved sulfate ($^{34}S/^{32}S$, $^{18}O/^{16}O$), total carbonate ($^{18}O/^{16}O$, $^{13}C/^{12}C$), and strontium ($^{87}Sr/^{86}Sr$). Moreover, sulfur isotope analysis was carried out on sulfides from the Chuquicamata porphyry copper deposit, that is located about twenty km from the geothermal field.

Hydrogen and oxygen isotopes of water

Chloride waters show δ^2H and $\delta^{18}O$ values of –71.8 to –64.7‰ and –3.6 to –5.5‰, respectively (Table 3; Fig. 11). These values are comparable to those of the samples collected in November 1968 (see Giggenbach, 1978 and references therein) from spring and well discharges with chloride concentration higher than 5000 mg/l. The analyzed sulfate springs show higher δ^2H and $\delta^{18}O$ values, with –49‰ and –2.1‰ respectively, which are within the range reported in the Giggenbach's paper (1978). Meteoric waters have δ^2H and $\delta^{18}O$ values respectively of –57.6 to –46.5‰ and –8.8 to –6.8‰, and include local cold springs, a recent snow sample from the area and the Rio Tucle stream upwards of any visible geothermal mani-

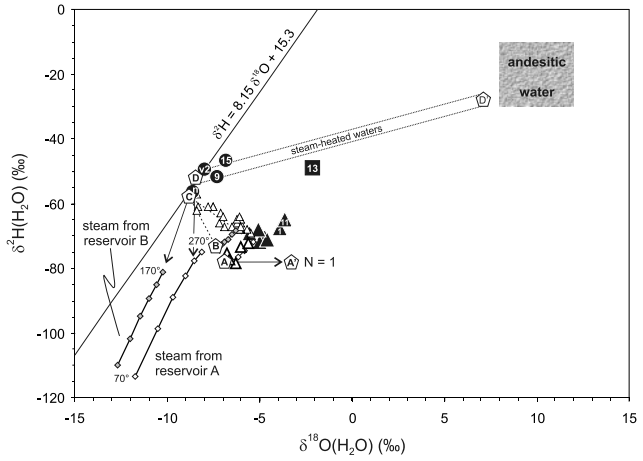

Fig. 11. δ^2H vs. $\delta^{18}O$ relation for new (hot and cold waters from this work; filled symbols) and previous (hot chloride water from Giggenbach, 1978; open symbols) data of El Tatio. The data are compared with the northern Chile meteoric water line (MWL, i.e., $\delta^2H = 8.15\ \delta^{18}O + 15.3$; Chaffaut et al., 1998), the isotopic effects from multistage-steam separation modeling for both the liquid and vapor phases and the isotopic trend depicted for steam-heated waters. The comparison also is made with the isotopic field of the magmatic (andesitic) water possibly involved in the geothermal system. A′ = maximum shift of fluid A by isotopic exchange with host rock; N = water to rock by volume ratio during interaction. See text for other details and references.

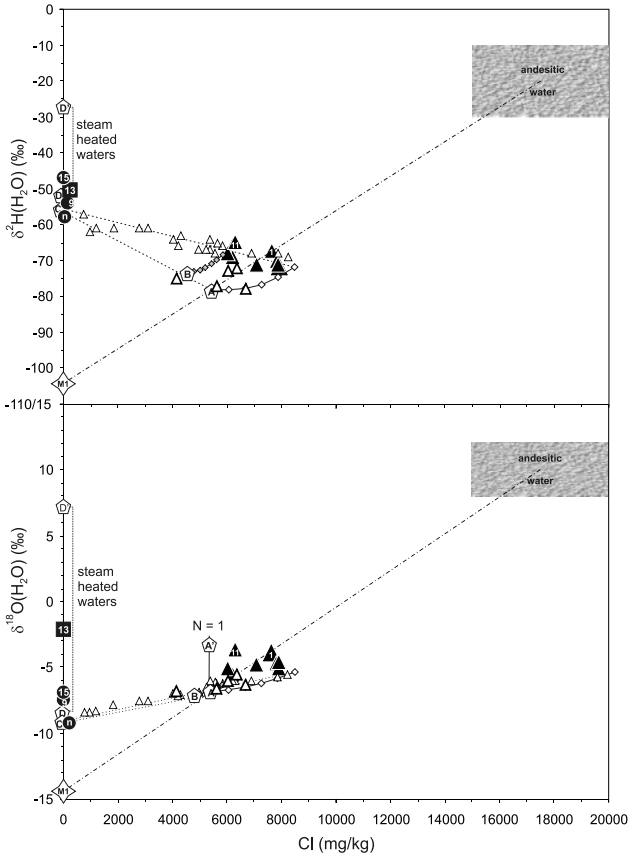

Fig. 12. δ^2H vs. Cl and $\delta^{18}O$ vs. Cl relations between the envisaged geothermal reservoirs A, B and C and the studied cold and hot waters of El Tatio. A binary mixing involving meteoric water and magmatic water is drawn for the main reservoir A. M1 = the meteoric end member in the mixed meteoric-magmatic model. Other symbols as in Fig. 11.

festation. Similar isotopic results were obtained by Giggenbach (1978) on meteoric waters, hot springs and wells.

All the available data from this work and the sodium-chloride waters from Giggenbach (1978) are compared in Fig. 11 with the meteoric water line of Chaffaut *et al.* (1998), the latter being based on precipitation (rain and snow) collected on the Altiplanos of northern Chile and southern Bolivia from 1994 to 1997 within an area located between 21.0–23.5°S and 67.0–68.5°W and at heights of 2,800 to 5,700 m. This meteoric line was preferred to that of Aravena *et al.* (1999), which refers to precipitation collected during 1984 to 1986 at heights of 2,380 to 4,250 m, which are on average lower than that of the El Tatio geothermal field. It is relevant that the Chaffaut *et al.*'s (1998) meteoric line is nearly identical to the one published by Gonfiantini *et al.* (2001) on precipitation along transects from the Amazon to the Altiplano in Bolivia during 1982 and 1986.

In the diagram, new and old data are undistinguishable, and apparently there is no reason for changing the Giggenbach's (1978) interpretation and conclusion in terms of isotopic composition of water sources and processes responsible for the thermal discharges (see Introduction). We only have to point out that: (1) local meteoric water samples fit well to the chosen line; (2) the meteoric water feeding the main geothermal reservoir is estimated to have δ^2H of –78‰ and $\delta^{18}O$ of –11‰; (3) secondary reservoirs (like the previously mentioned aquifer B) may form by mixing of primary water and meteoric local water, then feeding marginal springs; (4) the δ^2H and $\delta^{18}O$ of fluids from the reservoirs increase during the ascent toward the surface due to loss of vapor. In Figs. 11 and 12, multistage-steam separation from reservoirs A and B is depicted using updated fractionation factors and salinity corrections (Horita and Wesolowski, 1994; Horita *et al.*, 1995); (5) primary and secondary fluids mix with shallow meteoric groundwater before out flowing; the isotopic composition of this water is about –58‰ for hydrogen and –8.8‰ for oxygen; (6) this groundwater is slightly depleted in ^2H and ^{18}O relative to local meteoric water ($\delta^2H \sim -52$‰ and $\delta^{18}O \sim -8.5$‰; point D in the plot) by mixing with rising water vapor; and (7) steam-heated waters are mixtures between local

Table 3. Isotopic composition of H, O, S and C (in ‰) and Sr of waters and solutes at El Tatio

Sample	Description	Sampling date	$\delta^{18}O(H_2O)$ ‰ V-SMOW	$\delta^{2}H(H_2O)$ ‰ V-SMOW	^{3}H T.U.	$\delta^{13}C(DIC)$ ‰ PDB	$\delta^{18}O(DIC)$ ‰ PDB	$\delta^{34}S(SO_4)$ ‰ CDT	$\delta^{18}O(SO_4)$ ‰ V-SMOW	$^{87}Sr/^{86}Sr$
1	pool	17-Apr-2002	–3.90	–67.4	—	–18.3	–11.7	2.4	0.3	0.70884
2	geyser	17-Apr-2002	–4.71	–70.1	—	–12.0	–9.7	1.5	0.4	0.70893
3	geyser	17-Apr-2002	–4.77	–71.1	0.0 ± 0.5	–16.9	–12.7	—	—	0.70893
4	pool	17-Apr-2002	–4.90	–69.6	—	–12.0	–12.7	1.6	0.2	0.70894
5	geyser	17-Apr-2002	–5.03	–71.8	0.0 ± 0.4	–20.2	–10.0	2.0	1.2	0.70894
6	pool	17-Apr-2002	–4.60	–71.2	—	—	—	1.8	0.4	0.70890
7	pool	17-Apr-2002	—	—	—	—	—	—	—	0.70888
8	geyser	17-Apr-2002	–5.56	–69.1	0.0 ± 0.4	—	—	1.4	0.9	0.70896
9	cold spring	17-Apr-2002	–7.33	–51.8	2.2 ± 0.4	–14.4	–9.9	0.8	5.6	—
10	geyser	17-Apr-2002	–5.10	–68.1	—	–9.2	–5.9	2.6	1.4	0.70888
11	pool	18-Apr-2002	–3.63	–64.7	0.0 ± 0.4	–14.9	–12.4	2.6	1.1	0.70876
13	geyser	18-Apr-2002	–2.11	–49.0	0.3 ± 0.4	—	—	–9.7	3.5	—
15	Tucle stream	18-Apr-2002	–6.85	–46.5	—	—	—	4.4	9.7	0.70840
n	snow	29-Mar-2002	–8.77	–57.6	3.3 ± 0.6	—	—	—	—	—
v2	cold spring	29-Mar-2002	–7.96	–49.3	—	—	—	—	—	—

— = *not analysed.*

meteoric water and gases from the deep reservoir, and their distinct isotopic behavior is governed by kinetic effects during evaporation at very shallow levels. According to Giggenbach and Stewart (1982), the slope (S) of the straight line fitting steam-heated water samples on a δ^2H-$\delta^{18}O$ plot should be:

$$S = (\delta^2H_{si} - \delta^2H_{wi} + \varepsilon_{2H})/(\delta^{18}O_{si} - \delta^{18}O_{wi} + \varepsilon_{18O})$$

where the subscripts si and wi refer to the steam entering the pool and the local groundwater, respectively; ε is the kinetic isotope factor, which is close to 50‰ for hydrogen and 16‰ for oxygen. Considering the isotopic compositions of the steam leaving the reservoir A at 270°C and the reservoir B at 170°C, slopes of 1.4 to 1.5 are calculated (see Fig. 11). The slope refers to the line connecting the data points of local meteoric water (point D in the graph) and shallow meteoric groundwater heated by rising gases and then undergoing evaporation and related isotopic effects with a maximum enrichment in ^2H and ^{18}O (point D′ in the graph) as calculated following the Giggenbach and Stewart's (1982) procedure. The only analysed sulfate water (geyser 13) does not fit the line, probably due to a contribution of sodium-chloride water to the aquifer. On the other hand, the sodium-chloride springs 1 and 11 can be interpreted as lying on mixing lines between a major geothermal component from depth and a minor steam-heated component as suggested by both Figs. 11 and 12.

However, some contributions to this hydrogeological model of the El Tatio system can be added thanks to Giggenbach's (1992) paper on the origin of the geothermal water along convergent plate boundaries, i.e., the $\delta^{18}O$ of –6.9‰ (–6.3‰ according to Youngman, 1984) attributed by Giggenbach (1978) to the water of the main geothermal reservoir of El Tatio would not be the result of isotopic exchange of the feeding meteoric water with rocks, but it may be interpreted as deriving from mixing of meteoric precipitation from the Andean Cordillera with andesitic-magmatic water. Based on Fig. 12, the involvement of andesitic water (as defined by Taran *et al.*, 1989 and Giggenbach, 1992) implies a meteoric recharge with a δ^2H of about –107‰ (nival precipitation). The corresponding $\delta^{18}O$ should be about –14.6‰. These values can be assigned to Andean meteoric precipitation at altitudes higher than 4000 m (e.g., Fritz *et al.*, 1979; Gonfiantini *et al.*, 2001). A proportion of about 32% of magmatic water can be calculated from the chloride contents of the end members (0 mg/l for precipitation and 17,500 mg/l for andesitic water; Giggenbach and Soto, 1992), to which a chloride content of 5,400 mg/l corresponds in the admixture.

The possible involvement of andesitic water (as modified primary magmatic water) along with meteoric water (possibly with δ^2H about –100‰) in the hydrothermal systems related to the Tertiary volcanism of Andes was understood by Kamilli and Ohmoto (1977), discussing the δ^2H (–55 to –48‰) and $\delta^{18}O$ (–2.7 to +0.1‰) values of the 270 ± 20°C thermal fluids that about 10 m.y. ago formed most of the multistage Finlandia Pb-Zn-Ag-Au vein in the Colqui district located in the volcanic belt of Peru. Considering the next section about sulfur isotopes, sphalerite, galena and pyrite from this major ore stage yielded $\delta^{34}S$ values of –3.0 to +1.0‰. More recently, a

meteoric-andesitic model was also proposed by Urzua *et al*. (2002) in order to explain the isotopic composition of the geothermal fluids of the Apacheta field in northern Chile (see Fig. 1).

Is andesitic water an ordinary component of the Andean hydrothermalism?

In the δ^2H-δ^{18}O diagram of Fig. 13 the data on alkali-chloride geothermal wells and springs of Chile at Apacheta (Urzua *et al*., 2002), Puchuldiza and Tuja (Mahon and Cusicanqui, 1980) and of Bolivia at Laguna Colorada-Sol de Mañana (Scandiffio and Alvarez, 1992) and Empexa (Scandiffio and Cassis, 1992) are compared with the isotopic field expected for andesitic water and with the isotopic composition estimated for the main reservoir at El Tatio (see previous section). A very good fitting is obtained. On one hand this fact suggests mixing between magmatic and meteoric water, and on the other excludes appreciable ^{18}O-shift phenomena due to water-rock interaction. The diagrams deals also with alkali-chloride waters from the Challapaca (Scandiffio *et al*., 1992), Tutupaca (Scandiffio *et al*., 1992; Barragan *et al*., 1999) and Rio Calientes (Barragan *et al*., 1999) and other thermal systems (Steinmüller, 2001) in Peru. Also for these waters a mixing line is obtained connecting the meteoric and the andesitic components. It is noteworthy that the two trend lines intersects in the andesitic water box at +10‰ for δ^{18}O and –20‰ for δ^2H, whereas meteoric recharges of different isotopic compositions are derived, i.e., δ^2H of –107‰ and δ^{18}O of –14.6‰ for the Chilean and Bolivian systems, and δ^2H of –137‰ and δ^{18}O of –18.8‰ for the Peruvian hydrothermal systems.

The δ^2H and the δ^{18}O values of fluids from the vein ore deposit at Colqui (Steinmüller, 2001) obey straightforwardly to the meteoric-magmatic model (Fig. 13). Values for the ore-forming fluids in the same deposit were also published by Kamilli and Ohmoto (1977) from a fluid inclusion study; some of these values do not fit the meteoric-magmatic relation, possibly because of substantial oxygen isotopic exchange with rocks under low water to rock conditions. In fact, a number of the highest ^{18}O-shifts correspond to mineral parageneses particularly rich in quartz.

Strontium isotopes

The ^{87}Sr/^{86}Sr ratios in chloride waters are in the range 0.70876 to 0.70896, with all but one values rather uniform between 0.70884 and 0.70896. The lowest ratio refers to spring 11, and may be related to some depletion in ^{87}Sr of the rocks leached out by the feeding water. The Rio Tucle shows a ^{87}Sr/^{86}Sr of 0.70840, this suggesting that the local meteoric water interacts with rocks which are on average depleted in ^{87}Sr with respect to the deeper ones. The whole spread of isotopic ratios are conceivably related to variable proportion of crustal-derived Sr in the rocks leached by fluids (Harmon *et al*., 1984; Thorpe *et al*., 1984), the rocks ranging in composition from andesite to dacite to rhyolite. In Fig. 14 our data set is compared with those of andesites and dacites from the

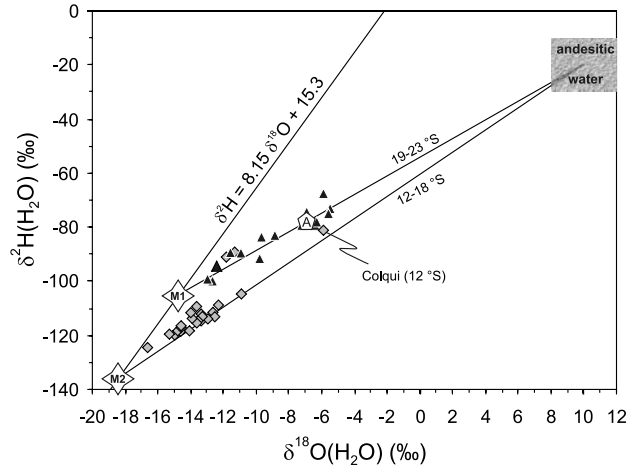

Fig. 13. δ^2H vs. δ^{18}O plot of hot springs and wells from Chilean-Bolivian (filled triangles) and Peruvian (grey diamonds) sodium-chloride geothermal waters, compared to the El Tatio reservoir A (pentagon) and andesitic water. The drawn mixing lines intersect into the andesitic water box. The data reported by Steinmüller (2001) for the epithermal ore vein of Colqui in Peru are also plotted, as they fit the involvement of andesitic water in the ore-forming fluids. M1 and M2 are meteoric end members involved in the recharges.

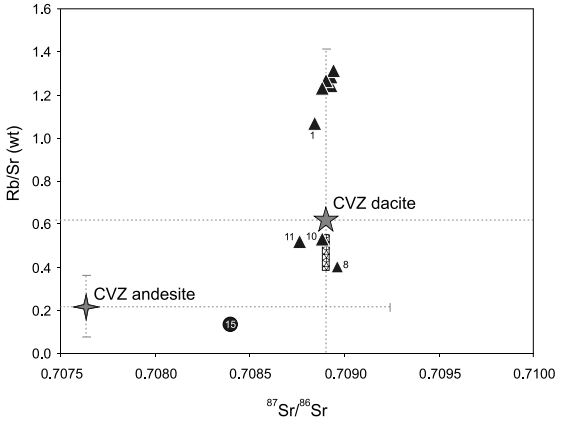

Fig. 14. Rb/Sr vs. ^{87}Sr/^{86}Sr plot for chloride hot (filled triangles) and cold (Rio Tucle; filled circle) waters from El Tatio, compared to mean values (±1σ) in dacites and andesites from the Central Volcanic Zone (CVZ) of Andes in northern Chile. The sketched box identifies the Rb/Sr ratios of dacites from the Rio Salado and Puripicar units in the El Tatio area (Youngman, 1984).

*Table 4. Summary of chemical and isotopic data from works on andesite and dacite specimens from the Central Volcanic Zone (CVZ) of Andes in northern Chile. N = number of samples; C.V. = (standard deviation/average)*100. See text for references.*

	Rb (ppm)	Sr (ppm)	Rb/Sr	$^{87}Sr/^{86}Sr$	$\delta^{18}O$ (‰)
CVZ andesite					
average	95	513	0.218	0.70763	8.58
st.dev.	42	175	0.143	0.00161	1.00
median	87	486	0.203	0.70714	8.45
N	63	63	63	54	32
C.V.	44	34	66	0.2	12
CVZ dacite					
average	156	346	0.617	0.70890	9.34
st.dev.	49	119	0.795	0.00238	1.57
median	158	320	0.481	0.70881	8.85
N	55	55	55	41	18
C.V.	31	34	129	0.3	17

Table 5. Parameters adopted in modeling the water-rock interaction effects in terms of $\delta^{18}O$ and $^{87}Sr/^{86}Sr$ values in selected hot chloride springs at El Tatio. CVZ = Central Volcanic Zone (CVZ) of Andes in Northern Chile. $C_r/C_{w,i}$ = rock/meteoric water ratio; $C_r/C_{g,i}$ = rock/geothermal water ratio (mixing between meteoric and andesitic waters).

	Oxygen	Strontium[a]
Meteoric water ($\delta_{w,i}$)	–11.45‰	+6.36‰[b]
Geothermal water (δ_g)	–6.90‰	+6.23‰[c]
CVZ dacite		
($\delta_{r,i}$)	+9.3‰[d]; +8.0‰[e]	+5.96‰
$C_r/C_{w,i}$	0.5	35,000
$C_r/C_{g,i}$	0.5	115[f]
Isotopic fractionation factors (270°C)		
$\Delta_{water-rock}$	–5.33‰[g]	0‰

[a] *Sr isotope δ-values are calculated as* $[(R_{sample}/0.7047) - 1] \times 1000$.
[b] *Data from McArthur (1994).*
[c] *Mix between 68% andesitic water and 32% meteoric water.*
[d] *Whole CVZ dacitic rocks.*
[e] *Plagioclase in CVZ dacitic rocks (Longstaffe et al., 1983).*
[f] *Sr content of geothermal reservoir estimated in 3 ppm.*
[g] *Water-albite fractionation factor (Zheng, 1993).*

Central Volcanic Zone (CVZ) of northern Chile (see Table 4 for a statistical summary of the data from Gardeweg *et al*., 1984; Harmon *et al*., 1984; De Silva *et al*., 1994; Schmitt *et al*., 2002; Lindsay *et al*., 2001). As expected, the chloride-springs are within the field depicted by the dacites, whereas the sulfate-spring matches the andesite field of values. These relations are in keeping with the volcano-stratigraphic units established to host the two aquifers. In particular, springs 10 and 11 from the reservoir B are related to the Tucle dacite unit, and their Rb/Sr ratios are within the range shown by the Rio Salado and Puripicar dacites (Youngman, 1984). These rocks host also the reservoir A, but the related springs display much higher Rb/Sr ratios. Probably, these springs are in equilibrium with Rb-rich illite. Obviously, the Sr isotopic composition of the mother rock is inherited by the interacting meteoric water and the neo-formed minerals (e.g., Tassinari *et al*., 1990). The Rio Tucle matches the field of CVZ andesites, as its feeding water very likely interacts with this type of rock in the subsoil.

Oxygen and strontium isotope exchange modeling between water and rock

Following the procedure described by Boschetti *et al*. (2003), the $^{87}Sr/^{86}Sr$ ratios of aqueous strontium were used in combination with the water $\delta^{18}O$ values to model the isotopic effects at 270°C on the meteoric recharge and on the meteoric-magmatic recharge as a consequence of their interaction with rocks in the main reservoir A. The equation describing the isotopic effects on water is:

$$\delta_{w,f} = [N\delta_{w,i} + (C_r/C_w)\delta_{r,i} + (C_r/C_w)(\delta_{r\text{-}w})/[N + (C_r/C_w)]$$

where N = water to rock by volume ratio, $\delta = \delta^{18}O$ or $\delta^{87}Sr$, w = water, r = rock, i = initial, f = final.

The parameters used in the model are reported in Table 5. The water $\delta^{18}O$ values are taken from Giggenbach (1978), i.e., –11.4‰ for the meteoric and –6.9‰ for the meteoric-magmatic. The concentration rock to water ratio (C_r/C_w) of 0.5 selected for oxygen applies to albite (48.7% oxygen)-water (88.9% oxygen) interaction and should be valid for the majority of volcanic rocks. The 35,000 figure for the strontium C_r/C_w ratio is a mean value for CVZ dacites.

Compared to the meteoric water-rock model (Fig. 15), the reservoir $\delta^{18}O(H_2O)$ value of –6.9‰ corresponds to a N value in the range 1.2 to 1.3, which in turn yields a $^{87}Sr/^{86}Sr$ ratio close to 0.70890 for the strontium in solution, that is practically indistinguishable from the dacite signature. This result does not concur to settle between meteoric water-magmatic water mixing and meteoric water-rock interaction as processes responsible for the geochemical characteristics of the El Tatio deep fluid. Probably, the interaction model cannot be applied here, as reasoned by Giggenbach (1993) with regard to the dynamic (andesitic) geothermal systems like El Tatio. Assuming that magmatic water is involved along with meteoric water, the post-mixing isotopic exchange with host rocks leads to a maximum $\delta^{18}O(H_2O)$ value of –3.3‰ (N = 1) for the main reservoir fluid applying an initial

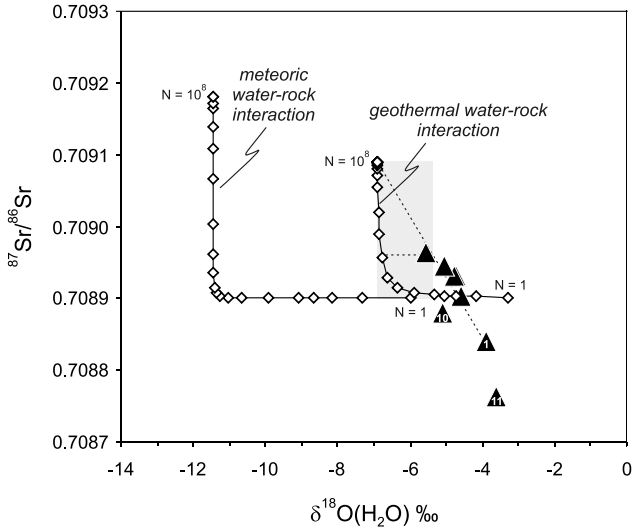

Fig. 15. Oxygen and strontium isotope composition of selected chloride hot waters from El Tatio, compared to the isotopic effects related to water-rock interaction in the main reservoir A at 270°C, as modelled under different water to rock ratios. Open diamonds and N represent variable water to rock by volume ratios. The modelling refers to the meteoric recharge and to the mixed meteoric-magmatic recharge. Dotted line interpolate the data on chloride springs 1 to 7 (excluding springs 10 and 11 as they should be fed by the secondary reservoir B) and the unaffected meteoric-magmatic geothermal fluid in the main reservoir. The grey box delimits the $\delta^{18}O(H_2O)$ range of –6.9‰ to –5.4‰ that can be assigned to the reservoir A, as a consequence of isotopic effects due to boiling. See text for more details.

Table 6. Sulfur isotopic composition of pyrite (Py), molybdenite (Mo) and secondary gypsum (G) from the Chuquicamata porphyry-copper mine

Sample	Main coexisting minerals[a]	$\delta^{34}S$ (‰)
Py-1	quartz, gypsum	0.2
Py-2	quartz, Fe-oxyde, molybdenite	0.6
Py-3	quartz, Fe-oxyde, molybdenite	0.4
Py-4	quartz, malachite	–0.6
Py-5	quartz, molybdenite, malachite	0.4
Py-6	quartz, molybdenite, malachite	–0.5
Py-7	quartz, Fe-oxyde, molybdenite	–0.4
Mo-1	molybdenite on quartz	0.4
G-1	lamellar gypsum on Py-1	–0.9

[a]*Analyzed by XRD.*

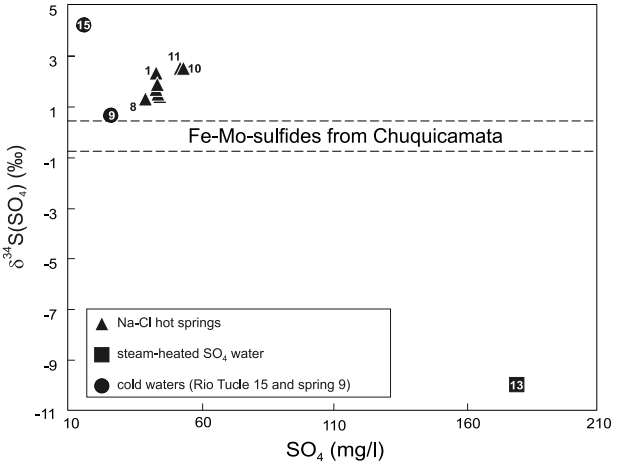

Fig. 16. Sulfur isotope composition of hot chloride (triangles) and sulfate (square) springs and cold waters (circles) at El Tatio, compared to Fe-Mo-sulfides from the porphyry copper mine of Chuquicamata, and relation with the sulfate concentration values.

$\delta^{18}O(H_2O)$ value of –6.9‰ for the mixture (Fig. 15). However, a $\delta^{18}O$ not higher than about –5.4‰ is allowed for the main reservoir fluid A by the evaporation model of Fig. 11. This could mean that springs with higher $\delta^{18}O$ values are contaminated by shallow steam-heated water. Back-extrapolation of a mixing line from spring 1 to the $\delta^{18}O$ value of –5.4‰ (Fig. 15) provides a fluid from reservoir A with a $\delta^{18}O$ of –6.9‰ and a $^{87}Sr/^{86}Sr$ ratio ranging from 0.70896 to 0.70909. These values would support the meteoric-magmatic origin of the geothermal fluid, also excluding significant isotopic exchange of the fluid with the reservoir rocks.

Sulfur and oxygen isotopes of sulfate

The sulfate from chloride waters displays quite uniform $\delta^{34}S$ between +0.8 and +2.6‰. This isotopic signature matches the one expected for Andean andesitic sulfur, that is in the range 0 to +4.4‰ (Taylor, 1986), and is consistent with those measured on pyrite and molibdenite samples from the Chuquicamata mine (–0.6 to +0.6‰, n = 8; Table 6). By the way, our data on Chuquicamata are well within the range of values measured in sulfides from several other porphyry copper deposits of the American Cordillera (–3 to +1‰ for sulfides, and +8 to +15‰ for sulfates; Ohmoto and Rye, 1979). Therefore, the sulfur in the geothermal waters of El Tatio derives from igneous sources, either from magmatic fluids or from dissolution of sulfides from the igneous host rocks. The slight ^{34}S-enrichment of the sulfate with respect to uncontaminated mantle sulfur (0‰) may be due to partitioning of sulfur isotopes between aqueous sulfate and sulfide species in the geothermal reservoir.

Sulfate from the analyzed steam-heated spring is notably depleted in ^{34}S with respect to chloride springs (Fig. 16). Its $\delta^{34}S$ value of –9.8‰ should be related to that of H_2S coming from the deep reservoir and undergoing oxidation in shallow air saturated water close to the

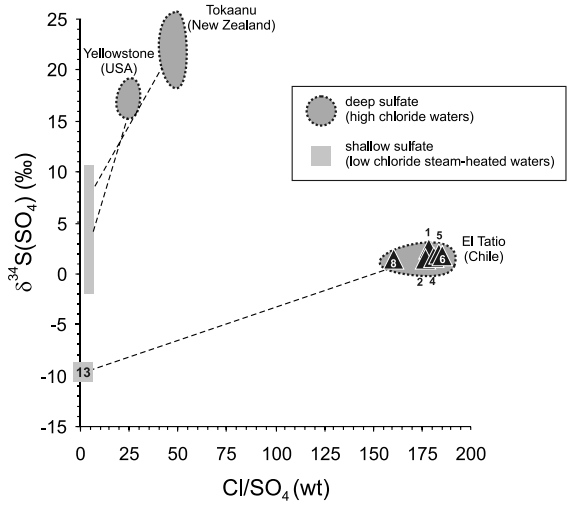

Fig. 17. Relations between $\delta^{34}S$ and Cl/SO_4 ratio in the hot high chloride waters supposed to derive directly from the main reservoir and the high sulfate, low chloride steam-heated water at El Tatio (this work), compared to samples from other geothermal systems in New Zealand and USA (Robinson, 1991).

surface. If complete oxidation takes place, the observed $\delta^{34}S$ appears to be not in isotopic equilibrium with sulfate in the chloride springs (mean $\delta^{34}S$ = +2.0‰), when the sulfate-sulfide isotopic fractionation of 11.8‰ presumed at El Tatio is compared with the one expected in the geothermal reservoir at 270°C (23‰; Ohmoto and Lasaga, 1982). Possibly, sulfur isotopic exchange between bisulfate and hydrogen sulfide in the reservoir does not reach equilibrium due to a rapid neutralization (within few hours?) of the acidity by rock alteration (see Kusakabe *et al*., 2000). However, the original $\delta^{34}S$ signature of the sulfate rising from the reservoir may have been lowered by substantial mixing with secondary sulfate from oxidation of H_2S at shallow levels. This interpretation would be supported by the $\delta^{34}S$ vs. Cl/SO_4 plot of El Tatio when compared to those of geothermal analogues elsewhere (Fig. 17) and for which mixing processes were concluded between a deep component and a shallow (steam-heated?) component (Robinson, 1991).

The $\delta^{34}S(SO_4)$ value of +1.8‰ measured in the cold spring (15.4 mg/l sulfate) flowing out at a higher elevation in the surroundings of the geothermal field is nearly identical to those of the hot springs. Oxidation of igneous sulfides in rocks passed through is most likely the main source of sulfate in this groundwater, along with minor isotopically indistinguishable atmospheric sulfate with a $\delta^{34}S$ value of about +2.5‰ (Castleman *et al*., 1974). A considerably higher $\delta^{34}S(SO_4)$ value of +5.4‰ is shown by the stream Rio Tucle (87.5 mg/l sulfate). This isotopic signature is consistent with those of streams and lakes in the High Andes, including the Rio Salado which commences at the El Tatio field (Rech *et al*., 2003). Probably, the sulfate in the Rio Tucle and other streams of the high Altiplano derives from the dissolution of sulfide and sulfate minerals like those associated to porphyry copper deposits, which are abundant in the Chilean Andes.

Table 7. Comparison between chemical (Na/K) and isotopic (SO_4-H_2O) thermometry applied to chloride springs at El Tatio. The isotopic temperatures are calculated assuming equilibrium with water from the main geothermal reservoir ($\delta^{18}O$ = –6.9‰). Values are in °C.

Sample	T(Na/K)[a]	T(SO_4-H_2O)[b]
1	232	227
2	228	225
4	237	229
5	235	211
6	245	225
Average	235 ± 6	223 ± 8

[a]*Chemical thermometer of Verma and Santoyo (1997).*
[b]*Isotopic thermometer of Seal et al. (2000).*

The $\delta^{18}O(SO_4)$ values of chloride springs are quite uniform in the range +0.2 to +1.4‰ (mean +0.7‰; n = 8). A considerably higher $\delta^{18}O(SO_4)$ value of +3.5‰ is observed in the analyzed sulfate spring. Much higher values (+5.6‰ and +9.7‰) were measured in the cold spring and Rio Tucle.

Based on the oxygen isotope fractionation factors between aqueous sulfate and water as reviewed by Seal *et al*. (2000), average equilibrium temperatures of 273 ± 18°C are calculated for chloride springs 1, 2, 4, 5, and 6, in keeping with the temperature of 270°C chemically estimated for the main reservoir A. The agreement is certainly misleading, as isotopic effects on the water-sulfate system are influenced by boiling, mixing and sulfide oxidation processes. Isotopic temperatures of 241 and 284°C are obtained in springs 10 and 11, these values being considerably higher than those given by Na/K or SiO_2 thermometry (154 and 175°C). Even if we apply the $\delta^{18}O$ of –7.2‰ obtained for the aquifer feeding these springs (reservoir B in Fig. 11), the resulting isotopic temperature of 202 and 207°C are still too high. In this aquifer, which should be fed by near neutral fluids rising from the main aquifer, sulfate-water oxygen isotope re-equilibration does not take place, basically due to the inverse correlation between isotopic exchange rate and pH (Chiba and Sakai, 1985). In Table 7, the thermometric estimates refer to springs supposed to be directly related to the main reservoir, the fluid $\delta^{18}O$ in the latter being –6.9‰. The agree-

ment is nearly perfect (the Student's t-test gives a significativity level of 0.01), even if the data are considerably lower than expected. Probably, the fluids underwent re-equilibration before discharge, and both thermometers record this event.

The oxygen isotope composition of sulfate from the only one analyzed sulfate steam-heated water distinguishes itself by the high $\delta^{18}O$ value of +3.5‰. It appears to be a disequilibrium signature (that provides an unrealistic isotopic temperature of 261°C), as also supported by the non-equilibrium conditions of the aqueous K-Na-Mg system in this springs (Fig. 3). The sulfate in this water basically derives from non-equilibrium oxidation of H_2S at shallow depth and low temperature, by which oxygen atoms from atmospheric O_2 and H_2O are incorporated (e.g., van Everdingen and Krouse, 1985).

Carbon and oxygen isotopes of total carbonate

The carbon isotopic composition $\delta^{13}C$ of aqueous carbonate (DIC) in analyzed chloride waters is largely variable between –20.1 to –9.2‰, with notable differences between individual springs from both the central part and the marginal part of the field. The oxygen isotope composition $\delta^{18}O$ is more uniform, with values between –12.7 to –5.9‰. The analyzed cold spring shows a $\delta^{13}C$ of –11.4‰ and a $\delta^{18}O$ of –9.9‰.

Possible sources of aqueous carbonate in the El Tatio geothermal system can be:

1. Soil-CO_2, that in northern Chile (Fritz *et al*., 1979) should have a $\delta^{13}C$ of about –18.5‰ in potential recharge areas with active vegetation (C_3-photosynthetic plants, with $\delta^{13}C \approx -23.5$‰; $P_{CO2} > 10^{-3.5}$ atm) at more than 3500 m above sea level. However, a lower $\delta^{13}C$ may be assigned to soil-CO_2 on Andes, e.g., –23‰ as observed in most C_3 landscapes (Cerling *et al*., 1991).

2. Rock carbonate, presumably with ^{13}C-content close to magmatic CO_2. Such carbonate could be dissolved by migrating groundwater, but its role in the carbon budget of the El Tatio waters cannot be established. As a matter of fact, the Andes are free of major carbonate sequences, but disseminated carbonate in the volcanic-magmatic rocks may be not a negligible source of carbonate species in solution, compared to the low concentration of bicarbonate in the analyzed springs (21.9 to 55.5 mg/l).

3. Volcanic-CO_2, that could play a role in the carbonate budget of the El Tatio waters. The $\delta^{13}C$ of this gas can be assumed to be in the range –8 to –5‰, even if some values up to –1‰ were measured in BAB (basalt-andesite-dacite association) CO_2 (Taylor, 1986). More recently, a $\delta^{13}C$ value of –3‰ was published by Poorter *et al*. (1989) for arc volcanic CO_2 from Indonesia.

These carbon sources should homogenize into the geothermal reservoir, where a fraction of the carbonate species may be reduced to methane, depending on the oxidation state. Therefore, the $\delta^{13}C$ of total carbon in the fluid should be in the range –23 to –3‰. If equilibrium or near to equilibrium between carbon-bearing species is assumed in the reservoir, the observed large spread of $\delta^{13}C$(DIC) values can be explained applying a $\delta^{13}C$ as low as –23‰ to total carbon in the reservoir (with bicarbonate enriched in 13C with respect to methane and depleted with respect to carbon dioxide; Ohmoto, 1972; see also Bannikova and Ryzhenko, 1985), and assuming an increase of the carbonate to methane ratio as a consequence of the increasing f_{O2} in the fluid after leaving the reservoir. The carbon isotope exchange between CO_2 and CH_4 is low at 270°C (>5 years for 90% equilibration at 350°C; Hulston, 1977; see also Hoefs, 1997), but it may be catalyzed by Fe-bearing phases in a Fischer-Tropsch-type reaction. Therefore, it is possible that carbon isotope equilibrium is approached in the reservoir, and afterwards oxidation of methane follows to different extents during ascent of the fluids without any appreciable isotopic re-equilibration, thus resulting in the range of $\delta^{13}C$ values measured for total carbonate in the springs. An alternative interpretation may be argued imaging equilibrium isotopic effects on the aqueous carbonate by open system degassing of CO_2 during uprising from the main reservoir (270°C) to the surface (50–80°C). By this process, released CO_2 is enriched in ^{13}C down to a temperature of 160°C (crossover point with respect to aqueous bicarbonate; Ohmoto and Rye, 1979), then becoming depleted in ^{13}C at lower temperature. Therefore, the observed $\delta^{13}C$ range of carbonate in the fluids can be explained by bulk degassing at temperatures lower than 160°C (at a total carbonate carbon $\delta^{13}C$ of about –23‰ in the reservoir), or at temperatures higher than 160°C if an initial $\delta^{13}C$ of about –3‰ is assumed for the total carbonate carbon. Probably, open system degassing is prevailing at lower temperatures and shallow levels, and it may concur to concentrate the ^{13}C in the solution during the travel to the surface.

If carbon isotope equilibrium is presumed in the geothermal reservoir, even more it should be achieved for the SO_4-H_2S pair (minimum time required for the attainment of 90% equilibrium should be of 4–5 years at 270°C and pH of 4 to 7; Ohmoto and Lasaga, 1982). In this case, the $\delta^{34}S$ signature of the sulfate in the reservoir is expected to be significantly higher than observed in the springs, if a $\delta^{34}S$ close to 0‰ is assumed for volcanic sulfur at El Tatio. Probably, most H_2S leaving the reservoir undergoes oxidation in the aqueous fluids during the ascent, thus providing sulfate with the observed isotopic signature.

The $\delta^{18}O$(DIC) values for analyzed hot and cold springs, compared to the oxygen isotope composition of water, do not yield oxygen isotope fractionations consistent with the outlet temperatures, and no relation exists

between the two parameters. The lack of an isotopic $\Delta^{18}O(HCO_3\text{-}H_2O)$ scale precludes to go deep into the question.

CONCLUSIONS

The main conclusions from this work are:

1. The chemistry of chloride springs are controlled by magma degassing and water-rock interaction processes. Sulfate springs are fed by shallow meteoric water heated by ascending gases. In keeping with the geodynamic setting and nature of the reservoir rocks, chloride water is rich in As, B, Cs, Li; on the other hand, sulfate water is enriched only in B relative to local meteoric water.

2. Alternatively to the merely meteoric model, chloride waters can be interpreted as admixtures of meteoric water and magmatic (circa andesitic) water, which moderately exchanges oxygen isotopes with rocks in distinct but connected reservoirs at chemical Na/K temperatures of about 270°C (main reservoir) and 170°C (secondary reservoir), and then suffered loss of vapor and eventually mixing with near-surface water. These chloride waters are devoid of tritium and can be classified as sub-modern (pre-1952).

3. Based on the enthalpy-chloride model, a chloride content of 5,400 mg/l is estimated in the main reservoir, for which δ^2H and $\delta^{18}O$ values respectively of –6.9‰ and –78‰ are calculated applying the multistage-steam separation isotopic effects between liquid and vapor. From these data, the meteoric recharge (Cl ≈ 0 mg/l) of the main reservoir should approach a composition of –107‰ in δ^2H and –14.6‰ in $\delta^{18}O$, when a magmatic water of δ^2H = –20‰, $\delta^{18}O$ = +10‰ and Cl = 17,500 mg/l is assumed.

4. The $^{87}Sr/^{86}Sr$ ratios of the hot springs are quite uniform (0.70876 to 0.70896), with values within the range observed for dacites of the Andean central volcanic zone, which derive from mantle magma contaminated by crustal rocks. A water $\delta^{18}O$-$^{87}Sr/^{86}Sr$ model is developed for the main geothermal reservoir, by which a meteoric-magmatic composition of the fluids is not excluded.

5. The uniform $\delta^{34}S(SO_4^{2-})$ values of +1.4 to +2.6‰ in the chloride waters agrees with a major deep-seated source for sulfur, possibly via hydrolysis in the geothermal reservoir of sulfur dioxide provided by magma degassing, followed by isotopic exchange between sulfate and sulfide in the main reservoir. This interpretation is supported by the largely negative $\delta^{34}S(SO_4^{2-})$ value in steam-heated water sulfate (–9.8‰) and mass-balance calculation, both of which exclude leaching at depth of igneous iron-sulfides with $\delta^{34}S$ near zero per mill.

6. All the $\delta^{13}C$ values of total carbonate in the chloride waters are negative, with variable values from –9.2 to –20.1‰, pointing to an important proportion of biogenic carbon in the fluids. The interpretation of these data is problematic. An alternative explanation is based on the combination of a $\delta^{13}C$ value as low as –23‰ for the total carbon in the main reservoir, with variably decreasing CO_2/CH_4 ratios in the rising fluids.

It may be of interest that the present work provides some support to the interrelation between the nearby El Tatio and Sol de Mañana geothermal fields, as proposed by Scandiffio and Alvarez (1992). Both systems lie on recent NW-SE trending normal faults, and both reservoirs should be in the Puripicar Ignimbrite, recharged from the Altiplano.

Acknowledgments—Many thanks are due to a number of people and particularly to Maria Soledad Bembow and Sergio Espinosa of the Departamento de Ciencias Geológicas de la Universidad Católica del Norte at Antofagasta for their valuable support during the stay in Chile (G.C.) and the sampling campaign. Special thanks to Giovanni Giannelli of the Institute of Geosciences and Earth Resources, CNR-Pisa, and to Enrico Dinelli of the Interdepartmental Centre for Research in Environmental Sciences of the Alma Mater Studiorum-University of Bologna, for their support in the elaboration of the thermodynamic database "data0.3245r46" associated to the Geochemist's Workbench® 4.0 software. The authors are grateful to the referees Carles Canet (Instituto de Geofísica, Universidad Nacional Autónoma de Mexico, UNAM) and Gilles Levresse (UNAM-Centro de Geociencias), for their useful comments and suggestions. We are also indebted to Kelevyn Youngman (Tauranga, New Zealand) for the permission to mention some results from his unpublished Master thesis. The chemical and isotopic analyses were carried out at the Department of Earth Sciences of the University of Florence (major elements), the Department of General and Inorganic Chemistry, Analytical Chemistry, Physical Chemistry of the University of Parma (trace elements), the Institute of Geosciences and Earth Resources of CNR at Pisa (stable isotopes) and the Department of Earth Sciences of the "La Sapienza" University of Rome (strontium isotopes).

REFERENCES

APHA-AWWA-WEF (1995) *Standard Methods for the Examination of Water and Wastewater*. 19th ed., American Public Health Association, American Water Works Association, Water Environment Federation.

Aravena, R., Susuki, O., Peña, H., Pollastri, A., Fuenzalida, H. and Grilli, A. (1999) Isotopic composition and origin of the precipitation in Northern Chile. *Appl. Geochem.* **14**, 411–422.

Bannikova, L. A. and Ryzhenko, B. N. (1985) Carbon and sulfur isotope ratios in the products of redox reactions under hydrothermal conditions (in the system CH_4-Na_2SO_4-NaCl-H_2O). *Geochem. Int.* **22**, 99–112.

Barragan, R. M., Arellano, V. M., Birkle, P., Portugal, M. and Dìaz, H. (1999) Isotopic composition and origin of the precipitation in northern Chile. *Appl. Geochem.* **14**, 411–422.

Bencini, A. (1977) Il dosaggio dei costituenti maggiori nelle

acque a bassa salinità. *Rend. Soc. It. Miner. Petrol.* **33**, 63–72 (in Italian).

Bethke, C. M. (2002) The Geochemist's Workbench. A User's Guide to Rxn, Act2, Tact, React, and Gtplot. Hydrogeology Program—University of Illinois. 236 pp.

Boschetti, T. (2003) Studio geochimico-isotopico di acque a composizione estrema e termali dell'Appennino Settentrionale. Ph.D. Thesis, Parma Univ., 358 pp. (in Italian).

Boschetti, T., Mangia, A., Mucchino, C. and Toscani, L. (2001) Determinazione simultanea di 17 elementi mediante ICP-MS in campioni di acque interagenti con rocce ultramafiche e basaltiche dell'Appennino Settentrionale. *Proc. XVI Congresso Nazionale di Chimica Analitica*, Chimica Analitica e Scienze del Mare, Portonovo, Ancona, 24–28 Settembre 2001 (in Italian).

Boschetti, T., Cortecci, G. and Bolognesi, L. (2003) Chemical and isotopic compositions of the shallow groundwater system of Volcano Island, Aeolian Archipelago, Italy: an update. *GeoActa* **2**, 1–34.

Cameron, J. F. (1967) Survey of systems for concentration and low background counting of tritium in water. *Radioactive Datings and Methods of Low-Level Counting*, 543–573, IAEA, Vienna.

Can, I. (2002) A new improved Na/K geothermometer by artificial neural networks. *Geothermics* **31**, 751–760.

Castleman, A. W., Munkelwitz, H. R. and Manowitz, B. (1974) Isotopic studies of the sulfur component of the stratospheric aerosol layer. *Tellus* **26**, 222–234.

Cerling, T. E., Solomon, D. K., Quade, J. and Bowman, J. R. (1991) On the isotopic composition of carbon in soil carbon dioxide. *Geochim. Cosmochim. Acta* **55**, 3403–3405.

Chaffaut, I., Coudrain-Ribstein, A., Michelot, J. L. and Pouyaud, B. (1998) Prècipitations d'altitude du Nord-Chili, origine des sources de vapeur et donnèes isotopiques. *Bull. Inst. Fr. Etudes andines* **27**, 367–384 (in French).

Chiba, H. and Sakai, H. (1985). Oxygen isotope exchange rate between dissolved sulphate and water at hydrothermal temperatures. *Geochim. Cosmochim. Acta* **49**, 993–1000.

Chiodini, G., Cioni, R., Guidi, M. and Marini, L. (1991) Chemical geothermometry and geobarometry in hydrothermal aqueous solutions: a theoretical investigation based on mineral-solution equilibrium model. *Geochim. Cosmochim. Acta* **55**, 2709–2727.

Chong, G., Pueyo, J. J. and Demergasso, C. (2000) Los yacimientos de boratos de Chile. *Revista geológica de Chile* **27**, 99–119.

Cusicanqui, H., Mahon, W. A. J. and Ellis, A. J. (1975) The geochemistry of the El Tatio geothermal field, Northern Chile. *Second United Nations Symposium on the Development and Utilization of Geothermal Resources*, 703–711, San Francisco.

De Silva, S. L. (1989) Geochronology and stratigraphy of the ignimbrites from the 21°30′ S to 23°30′ S portion of the Central Andes of northern Chile. *J. Volcanol. Geotherm. Res.* **37**, 93–131.

De Silva, S. L., Self, S., Francis, P. W., Drake, R. E. and Carlos Ramirez, R. (1994) Effusive silicic volcanism in the Central Andes: the Chao dacite and other young lavas of the Altiplano-Puna Volcanic Complex. *J. Geophys. Res.* **99**(B9), 17805–17825.

Déruelle, B. (1982) Petrology of the Plio-Quaternary volcanism of the South-Central and Meridional Andes. *J. Volcanol. Geotherm. Res.* **14**, 77–124.

Ellis, A. J. (1969) Survey for geothermal development in Northern Chile. Preliminary geochemistry report, El Tatio geothermal field. UNDP-Report.

Ellis, A. J. and Mahon, W. A. J. (1967) Natural hydrothermal systems and experimental hot-water/rock interactions (Part II). *Geochim. Cosmochim. Acta* **31**, 519–538.

Epstein, S. and Mayeda, T. (1953) Variations of the ^{18}O content of water from natural sources. *Geochim. Cosmochim. Acta* **4**, 213–224.

Ericksen, G. E., Vine, J. D. and Ballon, A. R. (1978) Chemical composition and distribution of lithium-rich brines in Salar de Uyuni and nearby salars in southwestern Bolivia. *Energy* **3**, 355–363.

Fehn, U. and Snyder, G. T. (2003) Origin of iodine and ^{129}I in volcanic and geothermal fluids from the North Island of New Zealand: implications for subduction zone processes. *Soc. Econ. Geologists, Special Publ.* **10**, 150–170.

Fournier, R. O. (1981) Application of water geochemistry to geothermal exploration and reservoir engineering. *Geothermal System: Principles and Case Histories* (Ribach, L. and Muffler, L. J. P., eds.), 109–143, John Wiley & Sons.

Fournier, R. O. and Truesdell, A. H. (1973) An empirical Na-K-Ca geothermometer for natural waters. *Geochim. Cosmochim. Acta* **37**, 1255–1275.

Fritz, P., Silva Heggings, C., Susuki, O. and Salati, E. (1979) Isotope hydrology in Northern Chile. *Proc. IAEA-UNESCO Symposium on Isotope Hydrology*, 19–23 June 1978, Neuherberg. IAEA, Vienna, Vol. 2, 525–544.

Gardeweg, M., Ishihara, S., Matsuhisa, Y, Shibata, K. and Terashima, S. (1984) Geochemical studies of Upper Cenozoic igneous rocks from the Altiplano of Antofagasta, Chile. *Chishitsu Chosasho Geppo* **35**, 547–563.

Geisemann, A., Jager, H. J., Krouse, H. P. and Brand, W. A. (1994) On line sulfur-isotope determination using elemental analyser coupled to a mass spectrometer. *Anal. Chem.* **66**, 2816–2819.

Giggenbach, W. F. (1978) The isotopic composition of waters from the El Tatio geothermal field, Northern Chile. *Geochim. Cosmochim. Acta* **42**, 979–988.

Giggenbach, W. F. (1988) Geothermal solute equilibria. Derivation of Na-K-Mg-Ca geoindicators. *Geochim. Cosmochim. Acta* **52**, 2749–2765.

Giggenbach, W. F. (1992) Isotopic shifts in waters from geothermal and volcanic systems along convergent plate boundaries and their origin. *Earth Planet. Sci Lett.* **113**, 495–510.

Giggenbach, W. F. (1993) Replay to comment by P. Blattner: "Andesitic water": a phantom of the isotopic evolution of water-silicate system. *Earth Planet. Sci Lett.* **120**, 519–522.

Giggenbach, W. F. and Soto, R. C. (1992) Isotopic and chemical composition of water and steam discharges from volcanic-magmatic hydrothermal systems of the Guanacaste Geothermal Province, Costa Rica. *App. Geochem.* **7**, 309–332.

Giggenbach, W. F. and Stewart, M. K. (1982) Processes controlling the isotopic composition of steam and water discharges from steam vents and steam-heated pools in geothermal areas. *Geothermics* **11**, 71–80.

Goguel, R. (1983) The rare alkalies in hydrothermal alteration at Wairakei and Broadlands, geothermal fields, N.Z. *Geochim. Cosmochim. Acta* **47**, 429–437.

Gonfiantini, R., Roche, M. A., Olivry, J. C., Fontes, J. Ch. and Zuppi, G. M. (2001) The altitude effect on the isotopic composition of tropical rains. *Chem. Geol.* **181**, 147–167.

Guest, J. E. (1969) Upper Tertiary ignimbrites in the Andean Cordillera of part of the Antofagasta Province, Northern Chile. *Geological Society of America Bulletin* **80**, 337–362.

Harmon, R. S., Barriero, B. A., Moorbath, S., Hoefs, J., Francis, P. W., Thorpe R. S., Déruelle, B., McHugh, J. and Viglino, J. A. (1984) Regional oxygen, strontium and lead isotope relationships in Late Cenozoic calc-alkaline lavas of the Andean Cordillera. *J. Geol. Soc.* **141**, 803–822.

Healy, J. (1974) Geological report on El Tatio geothermal field, Antofagasta province, Chile. UNDP-Report.

Healy, J. and Hochstein, M. P. (1973) Horizontal flow in hydrothermal systems. *N.Z. J. Hydrology* **12**, 71–82.

Hoefs, J. (1997) *Stable Isotope Geochemistry*. 4th ed., Springer-Verlag, 201 pp.

Honda, F., Mizutani, Y., Sugiura, T. and Oana, S. (1966) A geochemical study of iodine in volcanic gases. *Bull. Chem. Soc. Japan* **39**, 2690–2695.

Horita, J. and Wesolowski, D. J. (1994) Liquid-vapor feactionation of oxygen and hydrogen isotopes of water from the freezing to the critical temperature. *Geochim. Cosmochim. Acta* **58**, 3425–3437.

Horita, J., Cole D. R. and Wesolowski, D. J. (1995) The activity-composition relationships of oxygen and hydrogen isotopes in aqueous salt solutions: III. Vapor-liquid water equilibration of NaCl solutions to 350°C. *Geochim. Cosmochim. Acta* **59**, 1139–1151.

Hulston, J. R. (1977) Isotope work applied to geothermal systems at the Institute of Nuclear Sciences, New Zealand. *Geothermics* **5**, 89–96.

Jones, B. and Renaut, R. W. (1997) Formation of silica oncoids around geysers and hot springs at El Tatio, northern Chile. *Sedimentology* **44**, 287–304.

Kamilli, R. J. and Ohmoto, H. (1977) Paragenesis, zoning, fluid inclusion, and isotopic studies of the Finlandia vein, Colqui district, Central Peru. *Econ. Geol.* **72**, 950–982.

Kendall, C. and Coplen, T. B. (1985) Multisample conversion of water to hydrogen by zinc for stable isotope determination. *Anal. Chem.* **57**, 1437–1440.

Kharaka, Y. K. and Mariner, R. H. (1989) Chemical geothermometers and their application to formation waters from sedimentary basin. *Thermal History of Sedimentary Basins* (Naeser, N. D. and McCulloh, T. H., eds.), 99–117, Springer-Verlag.

Kharaka, Y. K., Lico, M. S. and Law L. M. (1982) Chemical geothermometers applied to formation waters, Gulf of Mexico and California basins. *Am. Assoc. Petrol. Geol. Bull.* **66**, 588.

Kornexl, B. E., Gehre, M., Höffling, R. and Werners, R. A. (1999) On-line $\delta^{18}O$ measurement of organic and inorganic substances. *Rapid Commun. Mass Spectrom.* **13**, 1685–1693.

Kusakabe, M., Komoda, Y., Takano, B. and Abiko, T. (2000) Sulfur isotopic effects in the disproportionation reaction of sulfur dioxide in hydrothermal fluids: implications for the $\delta^{34}S$ variations of dissolved bisulfate and elemental sulfur from active crater lakes. *J. Volcanol. Geotherm. Res.* **97**, 287–307.

Lahsen, A. and Trujillo, P. (1975) El Tatio Geothermal Field. *Proc. of the Second United Nations Symposium on the Development and Use of Geothermal Resources*, 157–178, San Francisco, California, May 20–29, 1975.

Lindsay, J. M., Schmitt, A. K., Trumbull, R. B., De Silva, S. L., Siebel, W. and Emmermann, R. (2001) Magmatic evolution of the La Pacana caldera system, central Andes, Chile: compositional variation of two cogenetic, large-volume ignimbrites. *J. Petrol.* **42**, 459–486.

Longstaffe, F. J., Claek, A. H., McNutt, R. H. and Zentilli, M. (1983) Oxygen isotopic composition of Central Andean plutonic and volcanic rocks, latitudes 26°–29° south. *Earth Planet. Sci. Lett.* **64**, 9–18.

Mahon, W. A. J. and Cusicanqui, H. (1980) Geochemistry of the Puchuldiza and Tuja hot springs, Chile. *N.Z. J. Sci.* **23**, 149–159.

Martin, J. B., Gieskes, J. M., Torres, M. and Kastner, M. (1993) Bromine and iodine in Peru margin sediments and pore fluids—implications for fluids origins. *Geochim. Cosmochim. Acta*, **57**, 4377–4389.

Matthews, S. J., Jones, A. P. and Gardeweg, M. C. (1994) Lascar Volcano, northern Chile; evidence for steady-state disequilibrium. *J. Petrol.* **35**, 401–432.

McArthur, J. M. (1994) Recent trends in strontium isotope stratigraphy. *Terra Nova* **6**, 331–358.

Mizutani, Y. and Rafter, T. A. (1969) Oxygen isotopic composition of sulphates-Part 5. Isotopic composition of sulphate in rain water, Gracefield, Lower Hutt, New Zealand. *N.Z. J. Sci.* **12**, 69–80.

Muñoz, M. and Hamza, V. (1993) Heat flow and temperature gradients in Chile. *Studia Geoph. Et Geod.* **37**, 315–348.

Nehring, N. L., Bowen, P. A. and Truesdell, A. H. (1977) Techniques for the conversion to carbon dioxide of oxygen from dissolved sulfate in thermal waters. *Geothermics* **5**, 63–66.

Nicholson, K. (1993) *Geothermal Fluids*. Springer-Verlag, 255 pp.

Ohmoto, H. (1972) Systematics of sulfur and carbon isotopes in hydrothermal ore deposits. *Econ. Geol.* **67**, 551–579.

Ohmoto, H. and Lasaga, A. C. (1982) Kinetics of reactions between aqueous sulfates and sulfides in hydrothermal systems. *Geochim. Cosmochim. Acta* **46**, 1727–1745.

Ohmoto, H. and Rye, R. O. (1979) Isotopes of sulfur and carbon. *Geochemistry of Hydrothermal Ore Deposits*, 2nd ed. (Barnes, H. L., ed.), 509–567, J. Wiley & Sons.

Parkhurst, D. L. and Appelo, C. A. J. (1999) User's guide to PHREEQC (version 2)—A computer program for speciation, batch reaction, one-dimensional transport and inverse geochemical calculations. U.S. Geological Survey, Water Resources Investigations Report 95-4259, Denver, Colorado. 312 pp.

Poorter, R. P. E., Varekamp, J. C., Van Bergen, M. J., Kreulen, R., Sriwana, T., Vroon, P. Z. and Wirakusumah, A. D. (1989)

The Sirung volcanic boiling spring: An extreme chloride-rich, acid brine on Pantar (Lesser Sunda Islands, Indonesia). *Chem. Geol.*, **76**, 215–228.

Rech, J. A., Quade, J. and Hart, W. S. (2003) Isotopic evidence for the source of Ca and S in soil gypsum, anhydrite and calcite in the Atacama Desert, Chile. *Geochim. Cosmochim. Acta* **67**, 575–586.

Reed, M. H. (1997) Hydrothermal alteration and its relationship to ore fluid composition. *Geochemistry of Hydrothermal Ore Deposits*, 3rd ed. (Barnes, H. L., ed.), 517–611, J. Wiley & Sons.

Risacher, F., Alonso, H. and Salazar, C. (2002) Hydrochemistry of two adjacent acid saline lakes in the Andes of northern Chile. *Chem Geol.* **187**, 39–57.

Robinson, B. W. (1991) Geothermal areas. *Stable Isotopes-Natural and Anthropogenic Sulphur in the Environment. SCOPE 43* (Krouse, H. R. and Grinenko, V. A., eds.), 245–247, J. Wiley & Sons.

Scandiffio, G. and Alvarez, M. (1992) Informe geoquímico sobre la zona geotérmica de Laguna Colorada, Bolivia. Estudios Geotérmicos con Técnicas Isotópicas y Geoquímicas en América Latina, 77–114, IAEA-TECDOC 641, Vienna.

Scandiffio, G. and Cassis, W. (1992) Geochemical report on the Empexa geothermal area, Bolivia. Estudios Geotérmicos con Técnicas Isotópicas y Geoquímicas en América Latina, 115–139, IAEA-TECDOC 641, Vienna.

Scandiffio, G., Verastegui, D. and Portilla, F. (1992) Geochemical report on the Challapalca and Tutupaca geothermal areas, Peru. Estudios Geotérmicos con Técnicas Isotópicas y Geoquímicas en América Latina, 345–375, IAEA-TECDOC 641, Vienna.

Schmitt, A. K., De Silva, S. L., Trumbull, R. B. and Emmermann, R. (2002) Magma evolution in the Purico ignimbrite complex, northern Chile: evidence for zoning of a dacitic magma by injection of rhyolitic melts following mafic recharge. *Contr. Mineral. Petrol.* **140**, 680–700.

Schwarz, G., Haak, V., Martínez, E. and Bannister, J. (1984) The electrical conductivity of the andean crust in northern Chile and southern Bolivia as inferred from magnetotelluric measurements. *J. Geophys.* **55**, 169–174.

Seal, R. R., II, Alpers, C. N. and Rye, R. O. (2000) Stable isotope systematics of sulfate minerals. *Reviews in Mineralogy & Geochemistry 40, Sulfate Minerals—Crystallography, Geochemistry and Environmental Significance*, 541–602, MSA, Washington, D.C.

Snyder, G. T. and Fehn, U. (2002) Origin of iodine in volcanic fluids: 129I results from the Central America Volcanic Arc. *Geochim. Cosmochim. Acta* **66**, 3827–3838.

Snyder, G. T., Fehn, U. and Goff, F. (2002) Iodine isotope ratios and halite concentrations in fluids of the Satsuma-Iwojima volcano, Japan. *Earth, Planets Space* **54**, 265–273.

Steinmüller, K. (2001) Modern hot springs in the southern volcanic Cordillera of Peru and their relationship to neogene epithermal precious-metal deposits. *J. South Am. Earth Sci.* **14**, 377–385.

Taran, Yu. A., Pokrovsky B. G. and Esikow, A. D. (1989) Deuterium and oxygen-18 in fumarolic steam and amphiboles from some Kamchatka volcanoes: "andesitic waters". *Dokl. Akad. Nauk. USSR* **340**, 440–443.

Taran, Yu. A., Hedenquist, J. W., Korzhinsky, M. A., Tkachenko, S. I. and Shmulovich, K. I. (1995) Geochemistry of magmatic gases from Kudryavy volcano, Iturup, Kuril Islands. *Geochim. Cosmochim. Acta* **59**, 1749–1761.

Tassinari, C., Lahsen, A., Munizaga, F., Sato, K. and Mori, P. E. (1990) Sr isotopic composition in fluid-rock systems in El Tatio and Puchildiza geothermal fields, northern Chile. *Geol. Soc. Australia* **27**, 99.

Taylor, B. E. (1986) Magmatic volatiles: isotopic variations of C, H and S stable isotopes in high temperature geological processes. *Reviews in Mineralogy* **16** (Valley, J. W., Taylor, H. P. and O'Neil, J. R., eds.), 185–225, Mineral. Soc. America.

Taylor, S. R. (1964) Abundance of chemical elements in the continental crust, a new table. *Geochim. Cosmochim. Acta* **28**, 1273–1285.

Thorpe, R. S., Francis P. W. and O'Callaghan, L. (1984) Relative roles of source composition, fractional crystallization and crustal contamination in the petrogenesis of Andean volcanic rocks. *Phil. Trans. R. Soc. London A* **310**, 675–692.

Urzua, L., Powell, T., Cumming, W. and Dobson, P. (2002) Apacheta, a new geothermal prospect in northern Chile. *Geothermal Resources Council 2002, Annual Meeting*, Reno, Nevada, 22–25 September 2002.

van Everdingen, R. O. and Krouse, H. R. (1985) Isotope composition of sulphates generated by bacterial and abiological oxidation. *Nature* **315**, 395–396.

Verma, M. P. (2001) Silica solubility geothermometers for hydrothermal systems. *Proc. of the 10th Int. Symp. on Water-Rock Interaction* (Cidu, R., ed.), Vol. 1, 349–352, Villasimius, Italy, June 10–15.

Verma, M. P. and Santoyo, E. (1997) New improved equations for Na/K, Na/Li and SiO_2 geothermometers by outlier detection and rejection. *J. Volcanol. Geotherm. Res*earch **79**, 9–24.

Youngman, K. J. (1984) Hydrothermal alteration and fluid-rock interaction in the El Tatio geothermal field, Antofagasta Province, Chile. Master Thesis, August 1984, The University of Auckland, Auckland, New Zealand, 123 pp.

Yuita, K. (1994) Overview and dynamics of iodine and bromine in the environment. *Japan Agricul. Res. Quarterly* **28**, 90–99.

Zheng, Y. F. (1993) Calculation of oxygen isotope fractionation in anhydrous silicate minerals. *Geochim. Cosmochim. Acta* **57**, 1079–1091.